Eur. Phys. J. C 54, 345–364 (2008)
DOI 10.1140/epjc/s10052-008-0528-3

THE EUROPEAN PHYSICAL JOURNAL C

Regular Article – Experimental Physics

Study of W-boson polarisations and triple gauge boson couplings in the reaction $e^+e^- \to W^+W^-$ at LEP 2

The DELPHI Collaboration

J. Abdallah[26], P. Abreu[23], W. Adam[55], P. Adzic[12], T. Albrecht[18], R. Alemany-Fernandez[9], T. Allmendinger[18], P.P. Allport[24], U. Amaldi[30], N. Amapane[48], S. Amato[52], E. Anashkin[37], A. Andreazza[29], S. Andringa[23], N. Anjos[23], P. Antilogus[26], W-D. Apel[18], Y. Arnoud[15], S. Ask[9], B. Asman[47], J.E. Augustin[26], A. Augustinus[9], P. Baillon[9], A. Ballestrero[49], P. Bambade[21], R. Barbier[28], D. Bardin[17], G.J. Barker[57], A. Baroncelli[40], M. Battaglia[9], M. Baubillier[26], K-H. Becks[58], M. Begalli[7], A. Behrmann[58], E. Ben-Haim[21], N. Benekos[33], A. Benvenuti[5], C. Berat[15], M. Berggren[26], D. Bertrand[2], M. Besancon[41], N. Besson[41], D. Bloch[10], M. Blom[32], M. Bluj[56], M. Bonesini[30], M. Boonekamp[41], P.S.L. Booth[24,†], G. Borisov[22], O. Botner[53], B. Bouquet[21], T.J.V. Bowcock[24], I. Boyko[17], M. Bracko[44], R. Brenner[53], E. Brodet[36], P. Bruckman[19], J.M. Brunet[8], B. Buschbeck[55], P. Buschmann[58], M. Calvi[30], T. Camporesi[9], V. Canale[39], F. Carena[9], N. Castro[23], F. Cavallo[5], M. Chapkin[43], Ph. Charpentier[9], P. Checchia[37], R. Chierici[9], P. Chliapnikov[43], J. Chudoba[9], S.U. Chung[9], K. Cieslik[19], P. Collins[9], R. Contri[14], G. Cosme[21], F. Cossutti[50], M.J. Costa[54], D. Crennell[38], J. Cuevas[35], J. D'Hondt[2], T. da Silva[52], W. Da Silva[26], G. Della Ricca[50], A. De Angelis[51], W. De Boer[18], C. De Clercq[2], B. De Lotto[51], N. De Maria[48], A. De Min[37], L. de Paula[52], L. Di Ciaccio[39], A. Di Simone[40], K. Doroba[56], J. Drees[58,9], G. Eigen[4], T. Ekelof[53], M. Ellert[53], M. Elsing[9], M.C. Espirito Santo[23], G. Fanourakis[12], D. Fassouliotis[12,3], M. Feindt[18], J. Fernandez[42], A. Ferrer[54], F. Ferro[14], U. Flagmeyer[58], H. Foeth[9], E. Fokitis[33], F. Fulda-Quenzer[21], J. Fuster[54], M. Gandelman[52], C. Garcia[54], Ph. Gavillet[9], E. Gazis[33], R. Gokieli[9,56], B. Golob[44,46], G. Gomez-Ceballos[42], P. Goncalves[23], E. Graziani[40], G. Grosdidier[21], K. Grzelak[56], J. Guy[38], C. Haag[18], A. Hallgren[53], K. Hamacher[58], K. Hamilton[36], S. Haug[34], F. Hauler[18], V. Hedberg[27], M. Hennecke[18], J. Hoffman[56], S-O. Holmgren[47], P.J. Holt[9], M.A. Houlden[24], J.N. Jackson[24], G. Jarlskog[27], P. Jarry[41], D. Jeans[36], E.K. Johansson[47], P. Jonsson[28], C. Joram[9], L. Jungermann[18], F. Kapusta[26], S. Katsanevas[28], E. Katsoufis[33], G. Kernel[44], B.P. Kersevan[44,46], U. Kerzel[18], B.T. King[24], N.J. Kjaer[9], P. Kluit[32], P. Kokkinias[12], C. Kourkoumelis[3], O. Kouznetsov[17], Z. Krumstein[17], M. Kucharczyk[19], J. Lamsa[1], G. Leder[55], F. Ledroit[15], L. Leinonen[47], R. Leitner[31], J. Lemonne[2], V. Lepeltier[21], T. Lesiak[19], W. Liebig[58], D. Liko[55], A. Lipniacka[47], J.H. Lopes[52], J.M. Lopez[35], D. Loukas[12], P. Lutz[41], L. Lyons[36], J. MacNaughton[55], A. Malek[58], S. Maltezos[33], F. Mandl[55], J. Marco[42], R. Marco[42], B. Marechal[52], M. Margoni[37], J-C. Marin[9], C. Mariotti[9], A. Markou[12], C. Martinez-Rivero[42], J. Masik[13], N. Mastroyiannopoulos[12], F. Matorras[42], C. Matteuzzi[30], F. Mazzucato[37], M. Mazzucato[37], R. Mc Nulty[24], C. Meroni[29], E. Migliore[48], W. Mitaroff[55], U. Mjoernmark[27], T. Moa[47], M. Moch[18], K. Moenig[9,11], R. Monge[14], J. Montenegro[32], D. Moraes[52], S. Moreno[23], P. Morettini[14], U. Mueller[58], K. Muenich[58], M. Mulders[32], L. Mundim[7], W. Murray[38], B. Muryn[20], G. Myatt[36], T. Myklebust[34], M. Nassiakou[12], F. Navarria[5], K. Nawrocki[56], R. Nicolaidou[41], M. Nikolenko[17,10], A. Oblakowska-Mucha[20], V. Obraztsov[43], A. Olshevski[17], A. Onofre[23], R. Orava[16], K. Osterberg[16], A. Ouraou[41], A. Oyanguren[54], M. Paganoni[30], S. Paiano[5], J.P. Palacios[24], H. Palka[19], Th.D. Papadopoulou[33], L. Pape[9], C. Parkes[25], F. Parodi[14], U. Parzefall[9], A. Passeri[40], O. Passon[58], L. Peralta[23], V. Perepelitsa[54], A. Perrotta[5], A. Petrolini[14], J. Piedra[42], L. Pieri[40], F. Pierre[41], M. Pimenta[23], E. Piotto[9], T. Podobnik[44,46], V. Poireau[9], M.E. Pol[6], G. Polok[19], V. Pozdniakov[17], N. Pukhaeva[17], A. Pullia[30], D. Radojicic[36], J. Rames[13], A. Read[34], P. Rebecchi[9], J. Rehn[18], D. Reid[32], R. Reinhardt[58], P. Renton[36], F. Richard[21], J. Ridky[13], M. Rivero[42], D. Rodriguez[42], A. Romero[48], P. Ronchese[37], P. Roudeau[21], T. Rovelli[5], V. Ruhlmann-Kleider[41], D. Ryabtchikov[43], A. Sadovsky[17], L. Salmi[16], J. Salt[54], C. Sander[18], A. Savoy-Navarro[26], U. Schwickerath[9], R. Sekulin[38], M. Siebel[58], A. Sisakian[17], G. Smadja[28], O. Smirnova[27], A. Sokolov[43], A. Sopczak[22], R. Sosnowski[56], T. Spassov[9], M. Stanitzki[18], A. Stocchi[21], J. Strauss[55], B. Stugu[4], M. Szczekowski[56], M. Szeptycka[56], T. Szumlak[20], T. Tabarelli[30], F. Tegenfeldt[53], J. Timmermans[32,a], L. Tkatchev[17], M. Tobin[24], S. Todorovova[13], B. Tome[23], A. Tonazzo[30], P. Tortosa[54], P. Travnicek[13], D. Treille[9], G. Tristram[8], M. Trochimczuk[56], C. Troncon[29], M-L. Turluer[41], I.A. Tyapkin[17], P. Tyapkin[17], S. Tzamarias[12], V. Uvarov[43], G. Valenti[5], P. Van Dam[32], J. Van Eldik[9], A. Van Lysebetten[2], N. van Remortel[16], I. Van Vulpen[9], G. Vegni[29], F. Veloso[23], W. Venus[38], P. Verdier[28], V. Verzi[39], D. Vilanova[41], L. Vitale[50], V. Vrba[13], H. Wahlen[58], A.J. Washbrook[24], C. Weiser[18], D. Wicke[9], J. Wickens[2], G. Wilkinson[36], M. Winter[10], M. Witek[19], O. Yushchenko[43], A. Zalewska[19], P. Zalewski[56], D. Zavrtanik[45], V. Zhuravlov[17], N.I. Zimin[17], A. Zintchenko[17], M. Zupan[12]

[1] Department of Physics and Astronomy, Iowa State University, Ames IA 50011-3160, USA
[2] IIHE, ULB-VUB, Pleinlaan 2, 1050 Brussels, Belgium

[3] Physics Laboratory, University of Athens, Solonos Str. 104, 10680 Athens, Greece
[4] Department of Physics, University of Bergen, Allégaten 55, 5007 Bergen, Norway
[5] Dipartimento di Fisica, Università di Bologna and INFN, Via Irnerio 46, 40126 Bologna, Italy
[6] Centro Brasileiro de Pesquisas Físicas, rua Xavier Sigaud 150, 22290 Rio de Janeiro, Brazil
[7] Inst. de Física, Univ. Estadual do Rio de Janeiro, rua São Francisco Xavier 524, Rio de Janeiro, Brazil
[8] Collège de France, Lab. de Physique Corpusculaire, IN2P3-CNRS, 75231 Paris Cedex 05, France
[9] CERN, 1211 Geneva 23, Switzerland
[10] Institut de Recherches Subatomiques, IN2P3 – CNRS/ULP – BP20, 67037 Strasbourg Cedex, France
[11] DESY-Zeuthen, Platanenallee 6, 15735 Zeuthen, Germany
[12] Institute of Nuclear Physics, N.C.S.R. Demokritos, P.O. Box 60228, 15310 Athens, Greece
[13] FZU, Inst. of Phys. of the C.A.S. High Energy Physics Division, Na Slovance 2, 182 21, Praha 8, Czech Republic
[14] Dipartimento di Fisica, Università di Genova and INFN, Via Dodecaneso 33, 16146 Genova, Italy
[15] Institut des Sciences Nucléaires, IN2P3-CNRS, Université de Grenoble 1, 38026 Grenoble Cedex, France
[16] Helsinki Institute of Physics and Department of Physical Sciences, P.O. Box 64, 00014 University of Helsinki, Finland
[17] Joint Institute for Nuclear Research, Dubna, Head Post Office, P.O. Box 79, 101 000 Moscow, Russian Federation
[18] Institut für Experimentelle Kernphysik, Universität Karlsruhe, Postfach 6980, 76128 Karlsruhe, Germany
[19] Institute of Nuclear Physics PAN,Ul. Radzikowskiego 152, 31142 Krakow, Poland
[20] Faculty of Physics and Nuclear Techniques, University of Mining and Metallurgy, 30055 Krakow, Poland
[21] Université de Paris-Sud, Lab. de l'Accélérateur Linéaire, IN2P3-CNRS, Bât. 200, 91405 Orsay Cedex, France
[22] School of Physics and Chemistry, University of Lancaster, Lancaster LA1 4YB, UK
[23] LIP, IST, FCUL – Av. Elias Garcia, 14-1^{o}, 1000 Lisboa Codex, Portugal
[24] Department of Physics, University of Liverpool, P.O. Box 147, Liverpool L69 3BX, UK
[25] Dept. of Physics and Astronomy, Kelvin Building, University of Glasgow, Glasgow G12 8QQ, UK
[26] LPNHE, IN2P3-CNRS, Univ. Paris VI et VII, Tour 33 (RdC), 4 place Jussieu, 75252 Paris Cedex 05, France
[27] Department of Physics, University of Lund, Sölvegatan 14, 223 63 Lund, Sweden
[28] Université Claude Bernard de Lyon, IPNL, IN2P3-CNRS, 69622 Villeurbanne Cedex, France
[29] Dipartimento di Fisica, Università di Milano and INFN-MILANO, Via Celoria 16, 20133 Milan, Italy
[30] Dipartimento di Fisica, Univ. di Milano-Bicocca and INFN-MILANO, Piazza della Scienza 3, 20126 Milan, Italy
[31] IPNP of MFF, Charles Univ., Areal MFF, V Holesovickach 2, 180 00, Praha 8, Czech Republic
[32] NIKHEF, Postbus 41882, 1009 DB Amsterdam, The Netherlands
[33] National Technical University, Physics Department, Zografou Campus, 15773 Athens, Greece
[34] Physics Department, University of Oslo, Blindern, 0316 Oslo, Norway
[35] Dpto. Fisica, Univ. Oviedo, Avda. Calvo Sotelo s/n, 33007 Oviedo, Spain
[36] Department of Physics, University of Oxford, Keble Road, Oxford OX1 3RH, UK
[37] Dipartimento di Fisica, Università di Padova and INFN, Via Marzolo 8, 35131 Padua, Italy
[38] Rutherford Appleton Laboratory, Chilton, Didcot OX11 OQX, UK
[39] Dipartimento di Fisica, Università di Roma II and INFN, Tor Vergata, 00173 Rome, Italy
[40] Dipartimento di Fisica, Università di Roma III and INFN, Via della Vasca Navale 84, 00146 Rome, Italy
[41] DAPNIA/Service de Physique des Particules, CEA-Saclay, 91191 Gif-sur-Yvette Cedex, France
[42] Instituto de Fisica de Cantabria (CSIC-UC), Avda. los Castros s/n, 39006 Santander, Spain
[43] Inst. for High Energy Physics, Serpukov P.O. Box 35, Protvino, (Moscow Region), Russian Federation
[44] J. Stefan Institute, Jamova 39, 1000 Ljubljana, Slovenia
[45] Laboratory for Astroparticle Physics, University of Nova Gorica, Kostanjeviska 16a, 5000 Nova Gorica, Slovenia
[46] Department of Physics, University of Ljubljana, 1000 Ljubljana, Slovenia
[47] Fysikum, Stockholm University, Box 6730, 113 85 Stockholm, Sweden
[48] Dipartimento di Fisica Sperimentale, Università di Torino and INFN, Via P. Giuria 1, 10125 Turin, Italy
[49] INFN,Sezione di Torino and Dipartimento di Fisica Teorica, Università di Torino, Via Giuria 1, 10125 Turin, Italy
[50] Dipartimento di Fisica, Università di Trieste and INFN, Via A. Valerio 2, 34127 Trieste, Italy
[51] Istituto di Fisica, Università di Udine and INFN, 33100 Udine, Italy
[52] Univ. Federal do Rio de Janeiro, C.P. 68528 Cidade Univ., Ilha do Fundão 21945-970 Rio de Janeiro, Brazil
[53] Department of Radiation Sciences, University of Uppsala, P.O. Box 535, 751 21 Uppsala, Sweden
[54] IFIC, Valencia-CSIC, and D.F.A.M.N., U. de Valencia, Avda. Dr. Moliner 50, 46100 Burjassot (Valencia), Spain
[55] Institut für Hochenergiephysik, Österr. Akad. d. Wissensch., Nikolsdorfergasse 18, 1050 Vienna, Austria
[56] Inst. Nuclear Studies and University of Warsaw, Ul. Hoza 69, 00681 Warsaw, Poland
[57] University of Warwick, Coventry CV4 7AL, UK
[58] Fachbereich Physik, University of Wuppertal, Postfach 100 127, 42097 Wuppertal, Germany

[†] deceased

Received: 22 November 2007 / Revised version: 14 December 2007 /
Published online: 2 February 2008 –

Abstract. A determination of the single W spin density matrix (SDM) elements in the reaction $e^+e^- \to W^+W^- \to l\nu q\bar{q}(l = e/\mu)$ is reported at centre-of-mass energies between 189 and 209 GeV. The data sample used corresponds to an integrated luminosity of 520 pb^{-1} taken by DELPHI between 1998 and 2000.

The single W SDM elements, $\rho^{W^\pm}_{\tau\tau'}$ ($\tau, \tau' = \pm 1$ or 0), are determined as a function of the W^- production angle with respect to the e^- beam direction and are obtained from measurements of the W decay products by the application of suitable projection operators, $\Lambda_{\tau\tau'}$, which assume the V-A coupling of the W-boson to fermions.

The measured SDM elements are used to obtain the fraction of longitudinally polarised Ws, with the result:

$$\frac{\sigma_{\rm L}}{\sigma_{\rm tot}} = 24.9 \pm 4.5(\text{stat}) \pm 2.2(\text{syst})\%$$

at a mean energy of 198 GeV. The SDM elements are also used to determine the triple gauge couplings $\Delta g_1^Z, \Delta\kappa_\gamma, \lambda_\gamma$ and $g_4^Z, \tilde{\kappa}_Z$ and $\tilde{\lambda}_Z$. For the CP-violating couplings the results of single parameter fits are:

$$g_4^Z = -0.39^{+0.19}_{-0.20}$$
$$\tilde{\kappa}_Z = -0.09^{+0.08}_{-0.05}$$
$$\tilde{\lambda}_Z = -0.08 \pm 0.07\,.$$

The errors are a combination of statistical and systematic errors. All results are consistent with the Standard Model.

1 Introduction

This paper reports on a study of W-boson polarisations and measurements of triple gauge couplings (TGC's) in the reaction $e^+e^- \to W^+W^-$, using data taken by the DELPHI experiment at LEP at centre-of-mass energies between 189 and 209 GeV. The amplitude of the reaction $e^+e^- \to W^+W^-$ results from t-channel neutrino and s-channel γ and Z exchange and is dominated by the lowest order, so-called CC03, diagrams (see Fig. 1). The s-channel diagrams contain trilinear γW^+W^- and ZW^+W^- gauge boson couplings whose possible deviations from the predictions of the Standard Model (anomalous TGC's), due to the effects of new physics, have been extensively discussed in the literature and are for instance described in references [1–6]. The decay angles of the charged lepton in the $W^-(W^+)$ rest frame are used to extract the single W CC03 spin density matrix (SDM) elements as a function of the W^- production angle with respect to the e^- beam direction. The method of projection operators described in reference [6] is used. Measurements of the SDM elements in the reaction $e^+e^- \to W^+W^-$ have been reported by OPAL [7].

The diagonal SDM elements have been used to obtain the differential cross-sections for longitudinally polarised W-bosons. The study of the longitudinal cross-section is particularly interesting as this degree of freedom of the W only arises in the Standard Model through the electroweak symmetry breaking mechanism. Measurements of the W polarisations at LEP have been reported previously by OPAL [7] and L3 [8]. The imaginary parts of the off-diagonal W^+ and W^- SDM elements should vanish in the Standard Model and are particularly sensitive to CP-violation [9]. Previous studies of CP-violation in the reaction $e^+e^- \to W^+W^-$ have been performed by ALEPH [10], DELPHI [11] and OPAL [7].

[a] e-mail: jan.timmermans@cern.ch

Fits were performed to SDM elements measured as a function of the W^- production angle with respect to the e^- beam direction in order to extract CP-conserving and CP-violating charged triple gauge boson couplings. In this paper the theoretical framework described in [1], based on the references given in [2, 3], is used. The effective Lagrangian containing only the lowest dimension operators (up to dimension six; terms of higher dimensions should be negligible at LEP energies [1]) and describing the most general Lorentz invariant WWV vertex, with $V = \gamma$ or Z, contains 14 terms with 14 corresponding couplings, $g_1^V, \kappa_V, \lambda_V, g_4^V, g_5^V, \tilde{\kappa}_V, \tilde{\lambda}_V$, representing the annihilation through the two virtual bosons (γ and Z). Assuming $\mathrm{SU(2)_L \times U(1)_Y}$ gauge invariance to be preserved, the following constraints between coupling constants are obtained [1, 4, 5]:

$$\Delta\kappa_Z = \Delta g_1^Z - \tan^2\theta_W \Delta\kappa_\gamma \quad (1)$$
$$\lambda_Z = \lambda_\gamma \quad (2)$$
$$\tilde{\kappa}_Z = -\tan^2\theta_W \tilde{\kappa}_\gamma \quad (3)$$
$$\tilde{\lambda}_Z = \tilde{\lambda}_\gamma \quad (4)$$

with $\Delta\kappa_Z = \kappa_Z - 1$, $\Delta\kappa_\gamma = \kappa_\gamma - 1$, $\Delta g_1^Z = g_1^Z - 1$ and θ_W the weak mixing angle.

Electromagnetic gauge invariance implies that $g_1^\gamma = 1$ and $g_5^\gamma = 0$ for on-shell photons ($q^2 = 0$) [1] . In the following the possible q^2-dependence of all the TGC's will be assumed to be negligible and we set[1] $g_1^\gamma = 1$ and assume that the CP-violating coupling $g_4^\gamma = 0$ and that $g_5^\gamma = g_5^Z = 0$ at all q^2. These last two coupling constants, although CP-conserving, correspond to the only terms vio-

[1] The parameters $g_1^\gamma, \kappa_\gamma$ and λ_γ are related to the charge Q_W, the magnetic dipole moment μ_W and the electric quadrupole moment q_W of the W^+ with: $Q_W = eg_1^\gamma$, $\mu_W = \frac{e}{2m_W}(g_1^\gamma + \kappa_\gamma + \lambda_\gamma)$ and $q_W = -\frac{e}{m_W^2}(\kappa_\gamma - \lambda_\gamma)$.

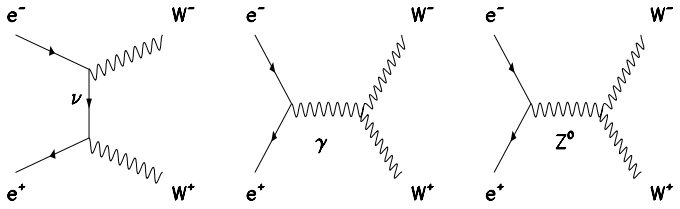

Fig. 1. CC03 diagrams

lating both C- and P-symmetry in the Lagrangian considered in this analysis.

With these assumptions, the number of independent coupling parameters can be reduced to six, three of which correspond to CP-conserving interactions ($\Delta g_1^Z, \Delta\kappa_\gamma$ and λ_γ), the remaining three being CP-violating ($g_4^Z, \tilde{\kappa}_Z$ and $\tilde{\lambda}_Z$). In the Standard Model (SM) all these parameters are expected to be zero at tree level. Hence Δg_1^Z and $\Delta\kappa_\gamma$ explicitly parameterise possible anomalous deviations of the couplings g_1^Z and κ_γ from their Standard Model values.

Triple gauge couplings have been measured by the four LEP experiments, ALEPH [10], DELPHI [12, 13], L3 [14] and OPAL [15]. The most recent results from DELPHI on CP-conserving TGC's [12, 13] were derived from data taken at centre-of-mass energies ranging from 189 to 209 GeV. Hadronic as well as leptonic decay channels of the W-bosons were considered using methods based on angular observables characterising both W production and decay. Measurements of CP-violating TGC's analogous to those described in this paper have been made by OPAL [16], while results from a different fit method have been published by ALEPH [10].

The selection of semi-leptonic $e^+e^- \to W^+W^- \to l\nu q\bar{q}(l = e, \mu)$ events and the corrections for efficiency, resolution and purity are given in Sect. 2. Section 3 discusses the determination of the single W SDM elements, the estimation of the fraction of longitudinally polarised Ws and the study of CP-violating effects on the imaginary elements. Section 4 is devoted to the estimation of the systematic errors on the SDM's. The TGC fits are described in Sect. 5. A global summary is given in Sect. 6.

2 Data sample and Monte Carlo simulation

For this analysis the data taken by DELPHI at centre-of-mass energies between 189 and 209 GeV were used. The DELPHI detector and its performance are described in reference [17, 18]. The data consist of events of the type $e^+e^- \to W^+W^- \to l\nu q\bar{q}(l = e, \mu)$. In order to take the energy dependence of the measurements into account, the data were grouped into three samples: 154 pb^{-1} taken in 1998 at 189 GeV, 218 pb^{-1} taken in 1999 at energies between 192 and 202 GeV (mean 198 GeV) and 149 pb^{-1} taken in 2000 at energies in the range 204 to 209 GeV (mean 206 GeV).

Events were selected in which one W decayed into a $e\nu$ or $\mu\nu$ pair while the other W decayed into a pair of quarks. These events are characterised by one isolated electron or muon, two hadronic jets and missing momentum coming from the neutrino. The major background comes from $q\bar{q}\tau\nu$ final states, from $q\bar{q}(\gamma)$ production and from neutral current four-fermion final states containing two quarks and two leptons.

After a loose preselection, an iterative discriminant analysis (IDA) was used to make the final selection. This part of the event selection is identical to the procedure used to measure the WW production cross-sections [19]. Events were selected with a cut on the output of the IDA, chosen to optimise the product of efficiency and purity for each channel. Events were first passed to the $q\bar{q}\mu\nu$ selection; if they were not selected, they were passed to the $q\bar{q}e\nu$ selection; if they were still not selected, they were then finally passed to the $q\bar{q}\tau\nu$ selection for possible inclusion or rejection. In this analysis only the events tagged as $q\bar{q}e\nu$ or $q\bar{q}\mu\nu$ were retained.

A three-constraint kinematic fit was then applied in which the masses of the two W candidates were constrained to be equal to a reference mass (80.35 GeV/c^2). A cut was applied on the χ^2 probability of this fit at 0.005. Events for which the angle between the lepton track and the beam axis was less than 20° were rejected to remove leptons with poor charge measurement.

The integrated luminosity used is 520 pb^{-1}, corresponding to data taking runs in which the subdetectors which were essential for this analysis were fully operational. A total of 1880 $l\nu q\bar{q}$ events was selected. The data were analysed separately for each of the three years. A breakdown of the collected statistics for different energies, as well as the mean energy for each sample, are given in Table 1, with other details.

The signal refers to the WW-like CC03 diagrams leading to $l\nu q\bar{q}$ final states [6]. The efficiencies and purities were estimated by Monte Carlo methods with the WPHACT [20, 21] program (charged and neutral current four-fermion events), and KK2F [22] ($q\bar{q}(\gamma)$ event generator) at energies of 188.6, 199.5 and 206.0 GeV. The hadronisation of quarks was simulated with the JETSET [23, 24] package. To account for the full $\mathcal{O}(\alpha)$ radiative corrections the generated charged current events were reweighted following the procedure described in [25]. The CC03 selection efficiency was around 70% while the purity was around 92%. Both were roughly energy independent as shown in Table 1.

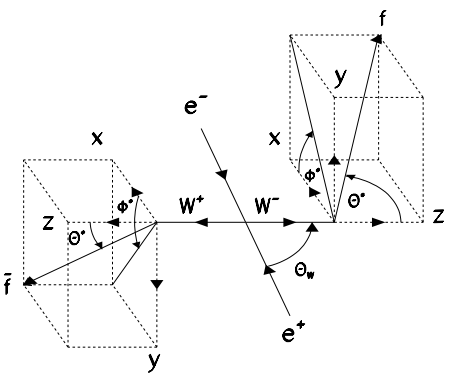

Fig. 2. Definition of the W^- production angle Θ_W and the lepton decay angles θ^* and ϕ^* in the rest frame of the W

Table 1. Statistics collected in each data taking year, Monte Carlo (MC) statistics used to calculate the detector corrections, efficiencies and purities. The Monte Carlo simulations have been performed at fixed centre-of-mass energies, as discussed in the text

data taking year	1998	1999	2000
mean energy (GeV)	189	198	206
energy range (GeV)	[188.5 - 189.]	[191.5 - 202.]	[204. - 209.]
luminosity (pb^{-1})	153.8	218.0	148.6
e+μ after all cuts (# evts)	520	838	522
efficiency electron evts	0.656	0.639	0.628
efficiency muon evts	0.787	0.759	0.743
average efficiency e+μ	0.721	0.699	0.685
average purity e+μ	0.923	0.917	0.914
energy of MC sample (GeV)	188.6	199.5	206
MC statistics CC (pb^{-1})	26 600	25 000	24 600
MC statistics NC (pb^{-1})	18 400	10 000	19 000
MC statistics $q\bar{q}(\gamma)$ (pb^{-1})	5000	5700	6300

To obtain the SDM elements the selected events were corrected for the acceptance, the angular resolutions and the sample purity. The correction factors were obtained from samples of simulated events with sizes given in Table 1.

The selection efficiency was calculated as a function of the W^- production angle $\cos\Theta_W$ and the lepton decay angles $\cos\theta^*$ and ϕ^*. The lepton decay angles are defined in the W rest frame as shown in Fig. 2. The efficiency is

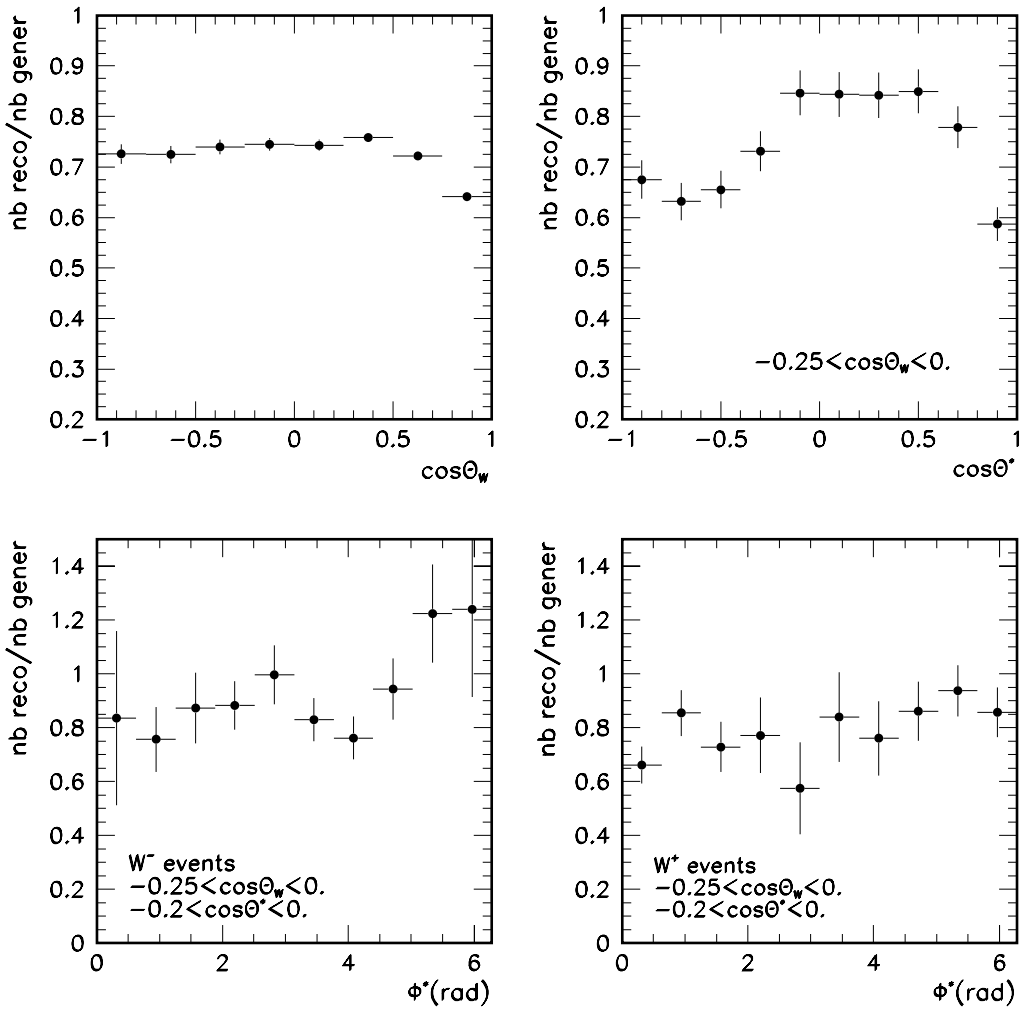

Fig. 3. Efficiency as function of $\cos\Theta_W, \cos\theta^*$ and ϕ^* at 199.5 GeV, obtained from simulated events

defined as the number of reconstructed events divided by the number of generated events in a given angular interval. Since the signal refers to the CC03 diagrams only, each event was reweighted by the ratio of the square of the matrix element for the CC03 diagrams only to the square of the matrix element for the full set of diagrams leading to $qqe\nu$ and $qq\mu\nu$ final states, including the full $\mathcal{O}(\alpha)$ radiative corrections. The events were divided in 8 equal bins of $\cos\Theta_W$, in 10 equal bins of $\cos\theta^*$ and in 10 equal bins of ϕ^*. The corrections were computed in each of these three-dimensional bins. The average number of generated events in a bin was 80 and about 7% of the bins were populated by less than 10 events. Examples of the efficiency distributions at 199.5 GeV are shown in Fig. 3.

The typical resolution on the measured $\cos\Theta_W$, after the 3C kinematic fit, was found to be 0.04, much smaller than the bin size of 0.25. For about 17% of the events the reconstructed $\cos\Theta_W$ deviates from the generated value by more than 0.125. Because of the definition of the selection efficiency as the convolution of efficiency and migration, correlations between neighbouring $\cos\Theta_W$ bins are expected after the correction procedure. A study of simulated events shows that between 70% and 90% of the events are reconstructed in the correct bin, and that the remaining events are nearly all reconstructed in the directly neighbouring intervals. The typical resolution on the measured $\cos\theta^*$ was 0.05, while it was 0.08 radians on the measured ϕ^*. This has to be compared to the bin widths of 0.2 and 0.628 radians respectively.

The purity with respect to CC03 e/μ production was calculated as a function of the three relevant angles with the same binning as used for the efficiencies. To estimate the signal contribution, the WW events were reweighted to obtain 'CC03 events' as explained above for the efficiency estimation. To estimate the background from $\tau\nu q\bar{q}$ and fully hadronic WW final states the events were reweighted to account for full O(α) radiative corrections. The small contribution of non-CC03 semi-leptonic e/μ events was also accounted as background. The other background contributions come from $q\bar{q}(\gamma)$ and neutral current four-fermion final states. Examples of the purity distributions at 199.5 GeV are shown in Fig. 4. Effective purities can become slightly greater

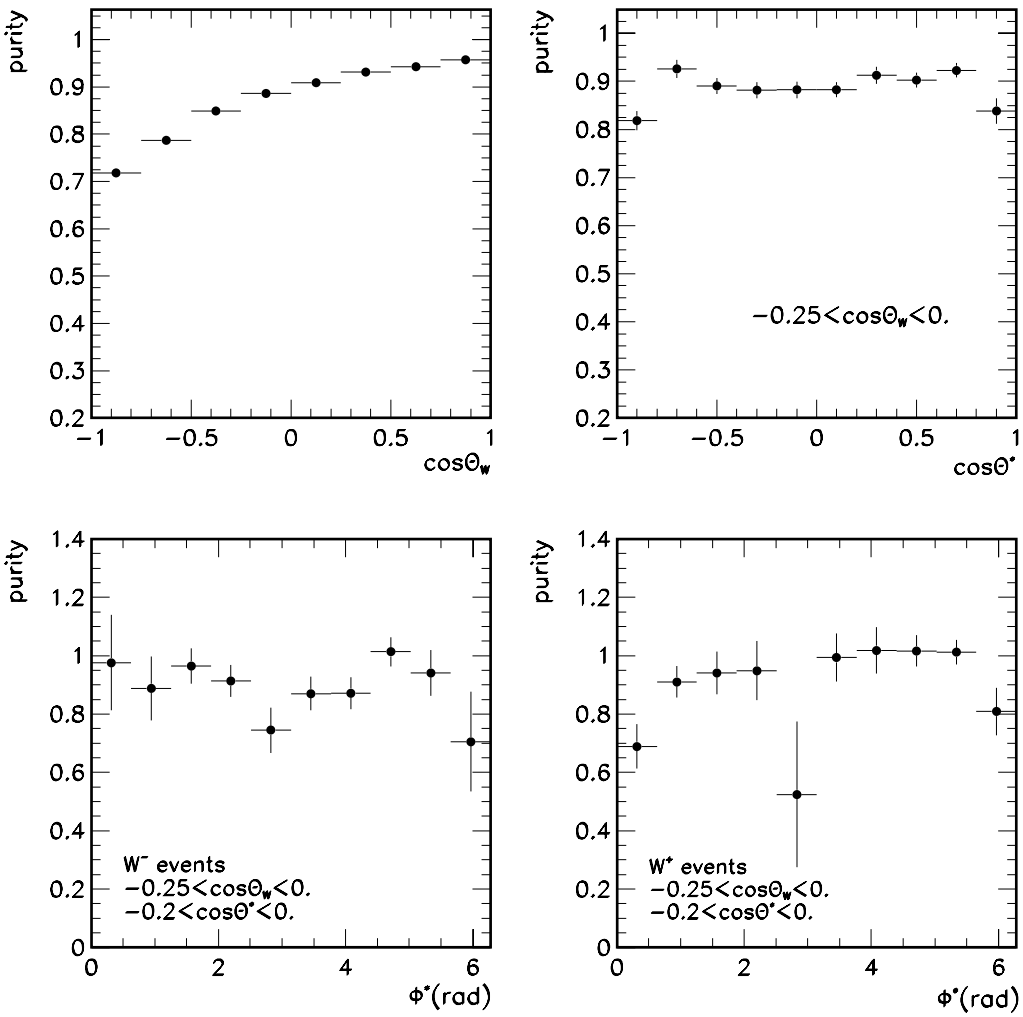

Fig. 4. Purity as function of $\cos\Theta_W$, $\cos\theta^*$ and ϕ^* at 199.5 GeV, obtained from simulated events

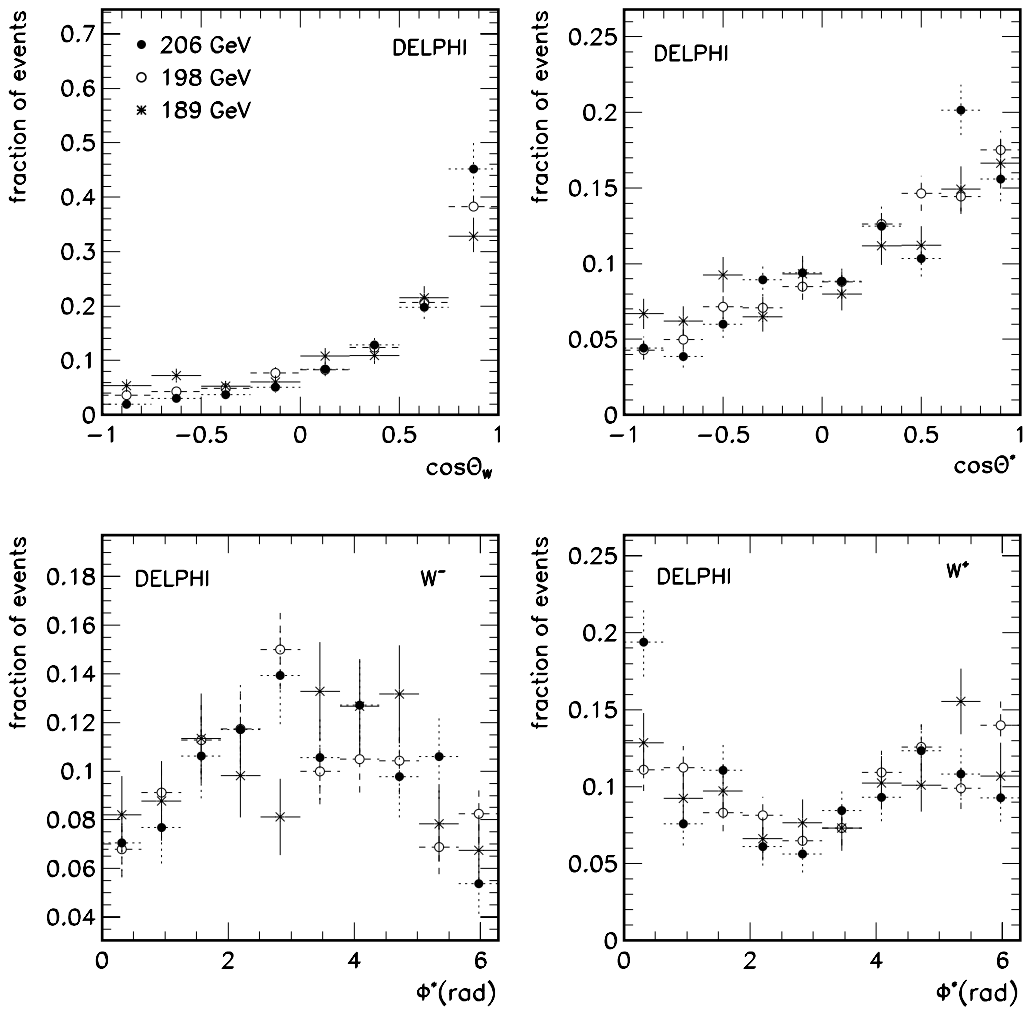

Fig. 5. Angular distributions, normalised to one and fully corrected, for data taken at 189 GeV, 198 GeV and 206 GeV

than 1 due to interference effects between CC03 and higher order diagrams affecting the CC03 reweighting procedure [25].

The fully corrected production and decay angle distributions obtained from the data are shown in Fig. 5 for the three data-taking years. The $\cos\Theta_W$ and $\cos\theta^*$ distributions for W^- and W^+ events, with the W decaying respectively in a negative or positive lepton, have been added together.

3 Single W spin density matrix and W polarisation

For events of the type

$$e^+(\lambda')\, e^-(\lambda) \to W^+(\tau_+)\, W^-(\tau_-)\,,$$

where $\lambda = \pm\frac{1}{2}$ ($\lambda' = -\lambda$) is the helicity of the electron (positron), $\tau_- = \pm 1, 0$ and $\tau_+ = \pm 1, 0$ are the helicities of the W^- and W^+, respectively, the two-body spin density matrix (SDM) is defined as [1, 4–6]:

$$\rho_{\tau_-\tau'_-\tau_+\tau'_+}(s, \cos\Theta_W) = \frac{\sum_\lambda F^{(\lambda)}_{\tau_-\tau_+} F^{*(\lambda)}_{\tau'_-\tau'_+}}{\sum_{\lambda\tau_-\tau_+} \left|F^{(\lambda)}_{\tau_-\tau_+}\right|^2} \qquad (5)$$

with $\cos\Theta_W$ the production angle of the W^- with respect to the e^- beam and $\mathrm{F}^{(\lambda)}_{\tau_-\tau_+}$ the amplitude for the production of a W^- with helicity τ_- and a W^+ with helicity τ_+. If only W^- decays are observed we have

$$\rho^{W^-}_{\tau_-\tau'_-}(s, \cos\Theta_W) = \sum_{\tau_+} \rho_{\tau_-\tau'_-\tau_+\tau_+}(s, \cos\Theta_W)\,,$$

$$\sum_{\tau_-} \rho^{W^-}_{\tau_-\tau_-} = 1\,.$$

In an analogous way, one has:

$$\rho^{W^+}_{\tau_+\tau'_+}(s, \cos\Theta_W) = \sum_{\tau_-} \rho_{\tau_-\tau_-\tau_+\tau'_+}(s, \cos\Theta_W)\,,$$

$$\sum_{\tau_+} \rho^{W^+}_{\tau_+\tau_+} = 1\,.$$

The differential cross-section for W^+W^- production with subsequent leptonic decay of the W^- can be written

as:

$$\frac{\mathrm{d}^3\sigma(e^+e^-\to W^+W^-\to W^+\ell^-\bar\nu)}{\mathrm{d}\cos\Theta_W\,\mathrm{d}\cos\theta^*\,\mathrm{d}\phi^*}\times\frac{1}{\mathrm{BR}}=$$
$$\frac{\mathrm{d}\sigma(e^+e^-\to W^+W^-)}{\mathrm{d}\cos\Theta_W}\left(\frac{3}{8\pi}\right)$$
$$\times\sum_{\tau_-\tau'_-}\rho^{W^-}_{\tau_-\tau'_-}(s,\cos\Theta_W)D_{\tau_-\tau'_-}(\theta^*,\phi^*)\,,$$

where the $D_{\tau_-\tau'_-}(\theta^*,\phi^*)$ functions describe the standard (V-A) decay of the W^-, (θ^*,ϕ^*) are the angles of the lepton in the W^- rest frame (see Fig. 2) and BR is the $W^-\to\ell^-\bar\nu$ branching fraction. The coordinate system in which these angles are defined is that of [4, 5] and corresponds to the one shown in Fig. 2. This representation of the differential cross-section in terms of the spin density matrix is independent of the specific form of the helicity amplitudes, i.e. of the specific form of the W^+W^- production process. The empirical determination of the SDM elements thus amounts to a model-independent analysis of this process.

A set of projection operators $\Lambda^{W^-}_{\tau_-\tau'_-}$ can be found [6] which isolate the corresponding $\rho^{W^-}_{\tau_-\tau'_-}$ contributions when integrated over the full lepton spectrum:

$$\rho^{W^-}_{\tau_-\tau'_-}=\frac{1}{\mathrm{BR}\times\frac{\mathrm{d}\sigma(e^+e^-\to W^+W^-)}{\mathrm{d}\cos\Theta_W}}$$
$$\times\int\frac{\mathrm{d}^3\sigma(e^+e^-\to W^+\ell^-\bar\nu)}{\mathrm{d}\cos\Theta_W\,\mathrm{d}\cos\theta^*\,\mathrm{d}\phi^*}$$
$$\times\Lambda^{W^-}_{\tau_-\tau'_-}(\theta^*,\phi^*)\,\mathrm{d}\cos\theta^*\,\mathrm{d}\phi^*\,.$$

The SDM elements for W^+ production are obtained in a similar way.

For a CP-invariant interaction, such as in the standard $\mathrm{SU(2)_L\times U(1)_Y}$ theory, the SDM elements of the produced

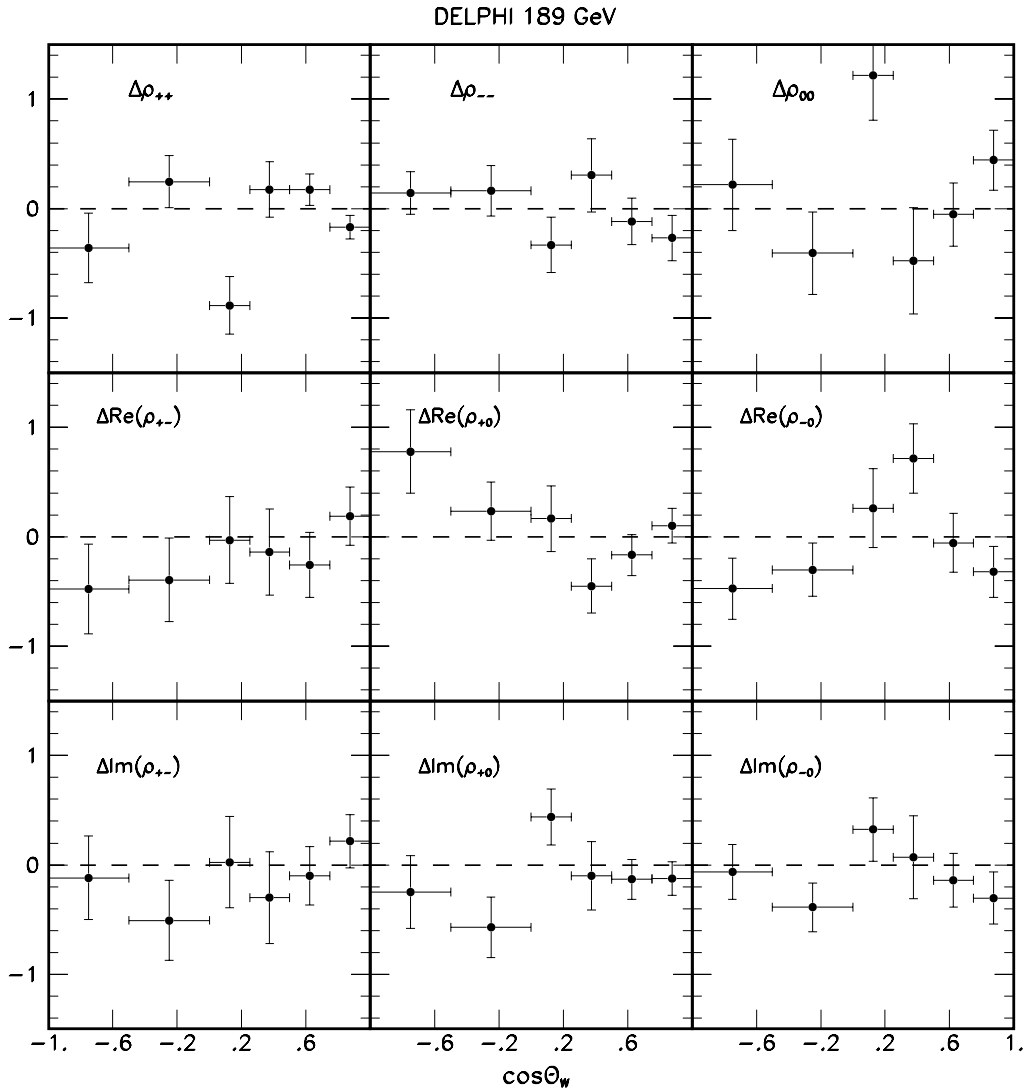

Fig. 6. Difference $\Delta\rho_{\tau\tau'}=\rho^{W^-}_{\tau\tau'}(s,\cos\Theta_W)-\rho^{W^+}_{-\tau-\tau'}(s,\cos\Theta_W)$ (see (6)), with statistical errors, measured with the data taken at 189 GeV, corrected for detector acceptance and sample purity as explained in the text

W^+ and W^- are related via [9]:

$$\rho^{W^-}_{\tau_-\tau'_-}(s,\cos\Theta_W) = \rho^{W^+}_{-\tau_--\tau'_-}(s,\cos\Theta_W)\,. \qquad (6)$$

The magnitude of any difference between the left-hand and right-hand sides of (6) constitutes a direct measure of the strength of a possible CP-violating interaction. At tree level, invariance under CPT transformations also implies the validity of relations (6) when applied to the real parts of the SDM, while for the imaginary parts, CPT invariance leads to the relation:

$$\mathrm{Im}\,\rho^{W^-}_{\tau_-\tau'_-} + \mathrm{Im}\,\rho^{W+}_{-\tau_--\tau'_-} = 0\,. \qquad (7)$$

Thus a violation of CP-invariance in WW production can best be investigated by looking for inequality of the imaginary parts of the SDM in (6), i.e. by testing the relations:

$$\mathrm{Im}\,\rho^{W^-}_{\tau_-\tau'_-} - \mathrm{Im}\,\rho^{W^+}_{-\tau_--\tau'_-} = 0\,. \qquad (8)$$

Relations (7) and (8) result in the fact that the imaginary parts of the SDM should vanish.

Experimentally the SDM elements were obtained from the relation

$$\rho^{W^\pm}_{\tau_-\tau'_-}(s,\cos\Theta_W) = \frac{1}{\sum_{j=1}^{N_i} w_j}\sum_{j=1}^{N_i} w_j\, \Lambda^{W^\pm}_{\tau_-\tau'_-}(\cos\theta^*_j,\phi^*_j)\,, \qquad (9)$$

where N_i is the number of selected events in a given $\cos\Theta_W$ bin. Each event was weighted with a correction factor w_j dependent on $(\cos\Theta_W,\cos\theta^*,\phi^*)$ as explained in Sect. 2, to account for detector acceptance, bin migration and sample purity.

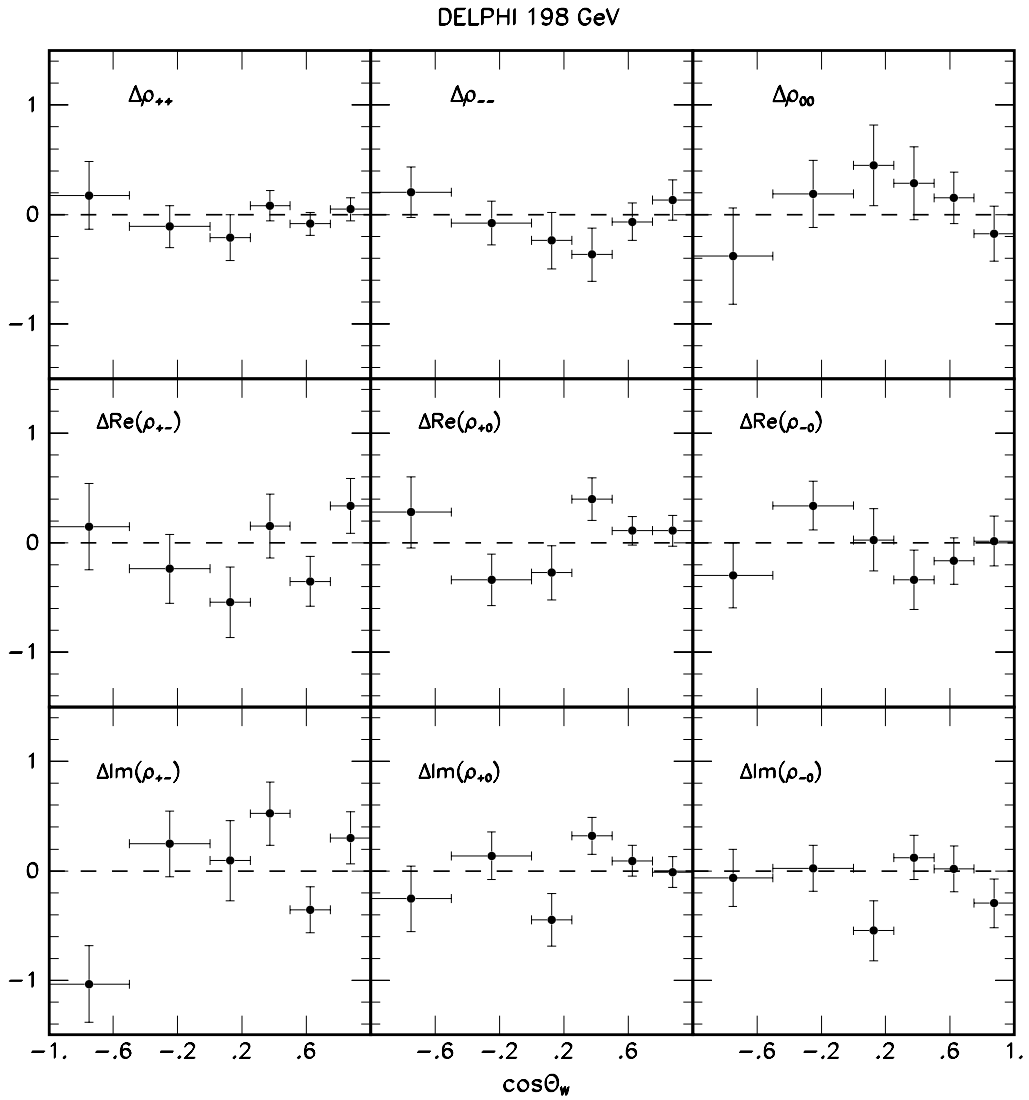

Fig. 7. Difference $\Delta\rho_{\tau\tau'} = \rho^{W^-}_{\tau\tau'}(s,\cos\Theta_W) - \rho^{W^+}_{-\tau-\tau'}(s,\cos\Theta_W)$ (see (6)), with statistical errors, measured with the data taken at 198 GeV, corrected for detector acceptance and sample purity as explained in the text

The event sample was divided into 8 equal bins of $\cos\Theta_W$. As the W^- production occurs mainly in the forward direction with respect to the e^- beam, and the experimental statistics available are rather restricted, 75% of the $\cos\Theta_W$ bins in the backward region have less than 20 events when the $\cos\Theta_W$ values are sampled in eight equal bins. From WPHACT Monte Carlo studies of a large number (250) of data-sized samples simulated at energies of 189, 200 and 206 GeV, it appears that the number of events per bin should be at least about 20 to allow a reliable extraction of triple gauge couplings from the data. In order to reach this goal, the SDM elements were redetermined in two equal-sized $\cos\Theta_W$ bins for W^- bosons produced in the backward region. Figures 6–8 show that the SDM elements computed for W^+ and W^- separately are compatible with relation (6) imposed by CP-invariance. Only statistical errors are displayed as systematic effects are expected to be small compared to statistical fluctuations (see Sect. 4) and are similar for W^+ and W^- bosons. The measurements of the SDM elements are shown in Figs. 9–11 for the three data samples taken in 1998, 1999 and 2000 separately. As the SDM elements computed for W^+ and W^- separately are compatible, CP-invariance is assumed in these plots and both the W^+ and W^- leptonic decays were used to compute the W^- SDM elements, based on relation (6). The predictions from Standard Model signal events (about $50\,000\,\mathrm{pb}^{-1}$ at each energy simulated with WPHACT) are also shown together with the results from the analytical calculations used in the TGC fits (see Sect. 5). The measured values agree with the SM expectation at all energies considered. Indeed, the χ^2 values for comparison with the analytical calculation, and taking into account the SDM elements in the 6 bins as shown in the Figs. 9 to 11, are respectively 45.3 (189 GeV), 43.5 (198 GeV) and 35.8 (206 GeV) for 48 degrees of freedom. In the calculation of the χ^2 the

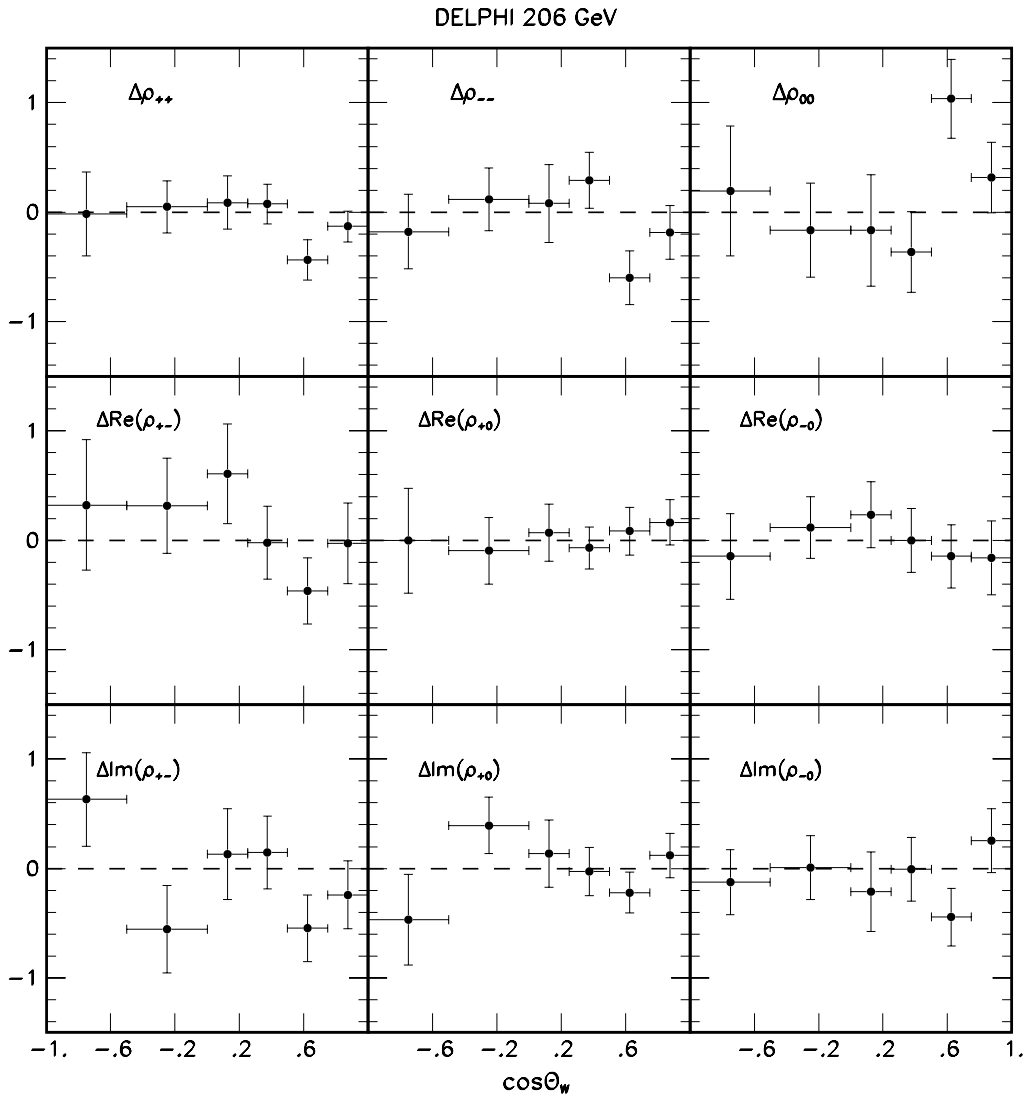

Fig. 8. Difference $\Delta\rho_{\tau\tau'} = \rho^{W^-}_{\tau\tau'}(s,\cos\Theta_W) - \rho^{W^+}_{-\tau-\tau'}(s,\cos\Theta_W)$ (see (6)), with statistical errors, measured with the data taken at 206 GeV, corrected for detector acceptance and sample purity as explained in the text

linear constraints on the diagonal elements were taken into account by removing the element ρ^{++}, and the full covariance matrix based on the statistical and systematic errors as explained in Sect. 5, was used. The corresponding χ^2 probabilities are 58.2%, 65.9% and 90.2% respectively.

In Figs. 9–11 a comparison is made of the CC03 SDM elements calculated with WPHACT (open dots) and those obtained with the expressions from [6] (full line), which do not include radiative corrections. It is seen that the two calculations agree well, which implies that the effect of radiative corrections is very small compared to the experimental errors.

The differential cross-section for the production of longitudinally polarised W-bosons is

$$\frac{\mathrm{d}\sigma_{\mathrm{L}}}{\mathrm{d}\cos\Theta_W} = \rho_{00}^{W}(\cos\Theta_W)\frac{\mathrm{d}\sigma}{\mathrm{d}\cos\Theta_W}\,. \qquad (10)$$

In this formula $\mathrm{d}\sigma/\mathrm{d}\cos\Theta_W$ is the differential cross-section after correction for detector acceptance and sample purity. The differential cross-sections were determined for the three energies considered. Figure 12 shows the luminosity weighted average of the measured differential cross-sections, together with the Standard Model predictions from WPHACT. The two distributions are in good agreement.

Integration yields the fraction of longitudinally polarised W-bosons:

$$f_{\mathrm{L}} = \sigma_{\mathrm{L}}/\sigma_{\mathrm{tot}}\,. \qquad (11)$$

Values of 18.7 ± 7.5 %, 27.4 ± 6.7 % and 27.6 ± 9.5 % are obtained from the data at 189, 198 and 206 GeV respectively, while values of 25.8 ± 0.3 %, 23.4 ± 0.3 % and 22.6 ± 0.3% are expected from the Standard Model Monte Carlo (about 50 000 pb^{-1} at each energy). These errors are statis-

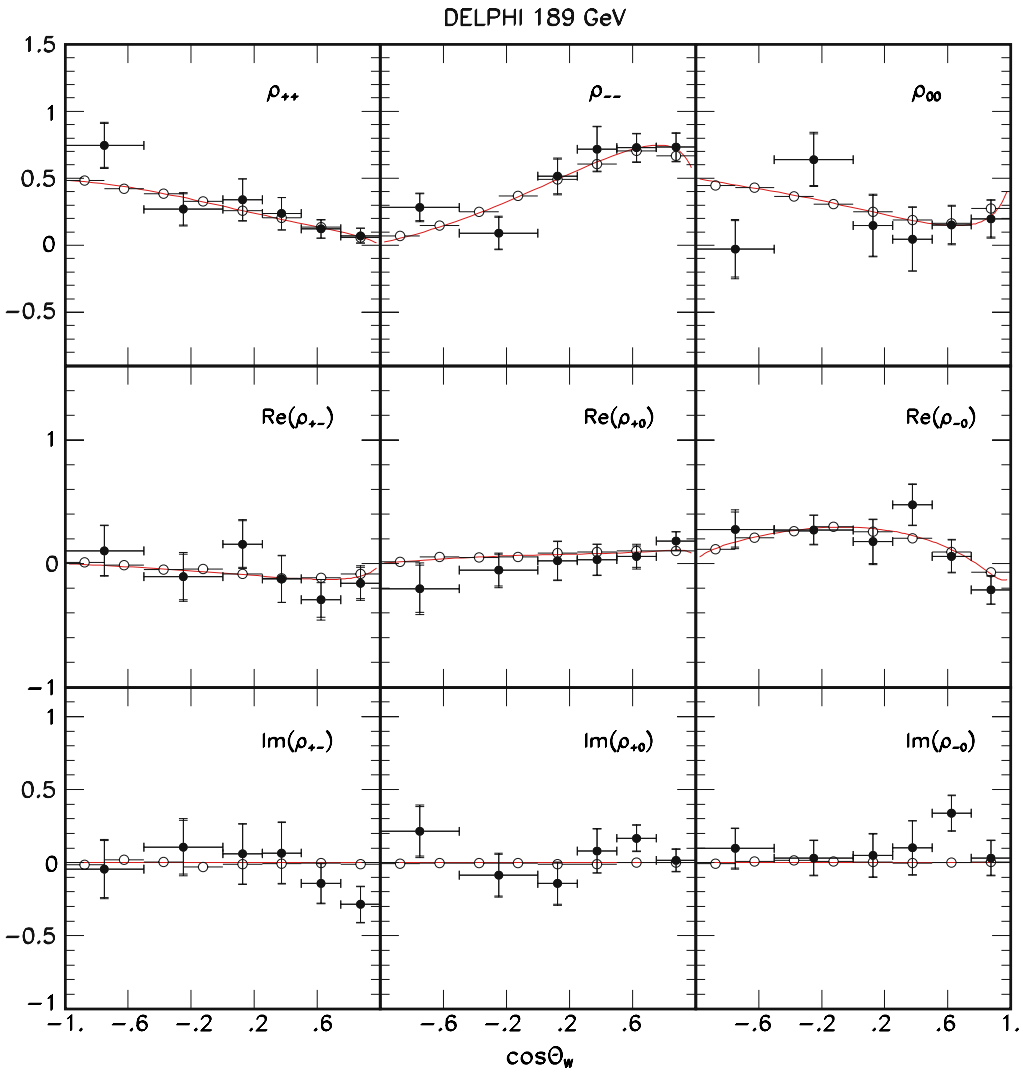

Fig. 9. Averages of W^+ and W^- SDM elements, with statistical and total errors, measured with the data taken at 189 GeV (*black dots*), corrected for detector acceptance and sample purity as explained in the text. The *full line* shows the tree level SM prediction calculated with the analytical expression from [6]. The *open circles* are the SM tree level predictions obtained with the WPHACT MC at generator level

tical only. The fraction of longitudinal W-bosons is shown as a function of the energy in Fig. 13. The luminosity weighted average over the three data samples is

$$\sigma_{\rm L}/\sigma_{\rm tot} = 24.9 \pm 4.5({\rm stat}) \pm 2.2({\rm syst})\% \qquad (12)$$

at a mean energy of 198 GeV. The systematic error is discussed in Sect. 4. This is in good agreement with the corresponding value of 23.9 ± 0.2 % expected from Standard Model Monte Carlo.

4 Systematic errors on the SDM elements

The systematic uncertainties in the measurements of the SDM elements were calculated as described below. The list of systematic errors considered for ρ_{00} is shown in Table 2 as an example. The systematic errors on the differential cross-section and on the fraction of longitudinally polarised W-bosons were estimated in the same way and are discussed at the end of this section.

1. Monte Carlo statistics. The detector corrections are binned in 8 bins in $\cos\Theta_W$, 10 bins in $\cos\theta^*$ and 10 bins in ϕ^*. Some bins have a low population of events which results in a large uncertainty in the correction factor. To estimate this effect on the SDM elements, the simulated data samples were divided in 9 subsamples of about $2600\,{\rm pb}^{-1}$ and detector corrections were computed for each subsample. The analysis was rerun on the data with each set of detector corrections and the differences of the new SDM elements with the SDM elements obtained with the standard corrections were computed. The standard deviation of the distributions

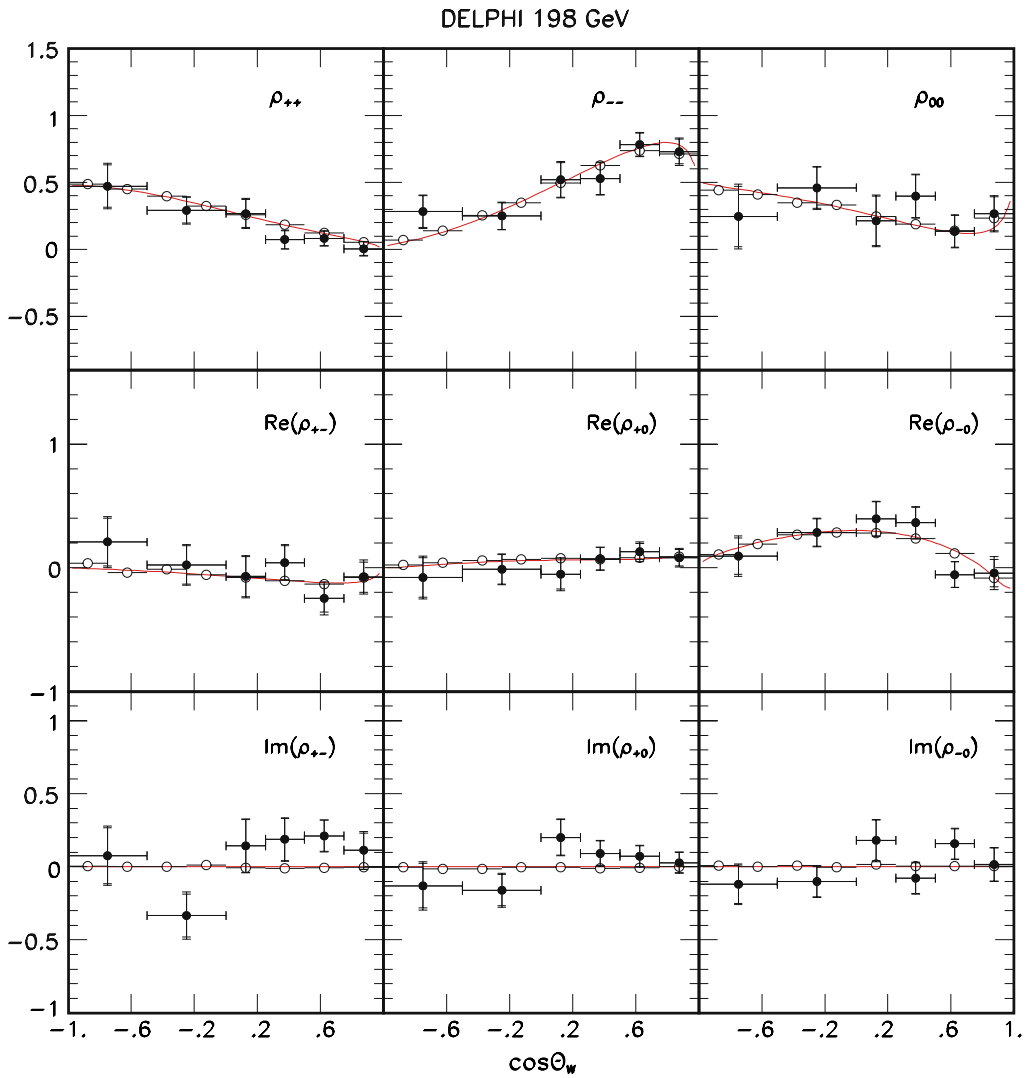

Fig. 10. Averages of W^+ and W^- SDM elements, with statistical and total errors, measured with the data taken at an energy of 198 GeV (*black dots*), corrected for detector acceptance and sample purity as explained in the text. The *full line* shows the tree level SM prediction calculated with the analytical expression from [6]. The *open circles* are the SM tree level predictions obtained with the WPHACT MC at generator level

of differences, corrected for the factor 9 difference in statistics between the subsamples and the full sample, was taken as the systematic error.

2. Signal and background cross-sections. The uncertainties on the signal and background cross-sections influence the purities. For the estimation of the systematic error arising from the uncertainty on the background cross-sections only the uncertainties on the $q\bar{q}(\gamma)$ and four-fermion neutral current cross-sections were taken into account, and were taken to be 5% [26]. The purities were recalculated with background cross-sections which were modified by plus and minus one standard deviation. The mean of the differences of the recomputed SDM elements and the standard elements was taken as systematic uncertainty.
   The uncertainty on the signal cross-section enters both in the denominator and the numerator and its effect is expected to be small. The purities were recalculated with signal cross-sections which were modified by plus and minus one standard deviation. The uncertainty on the signal cross-section was taken to be 0.5% , the theoretical error [26]. The mean of the differences of the recomputed SDM elements and the standard elements was taken as systematic uncertainty. These uncertainties are negligible at all energies considered.
3. Jet reconstruction, hadronisation modelling and migration of events between $\cos\Theta_W$ bins. The reconstruction of the hadronic jets influences the determination of the W production and decay angles and will hence lead to migration effects between bins in the $\cos\Theta_W$ distribution. On the other hand, the corrections for acceptance and purity are sensitive to the modelling of the hadronisation in the simulation. To estimate these effects, the differences between the SDM elements cal-

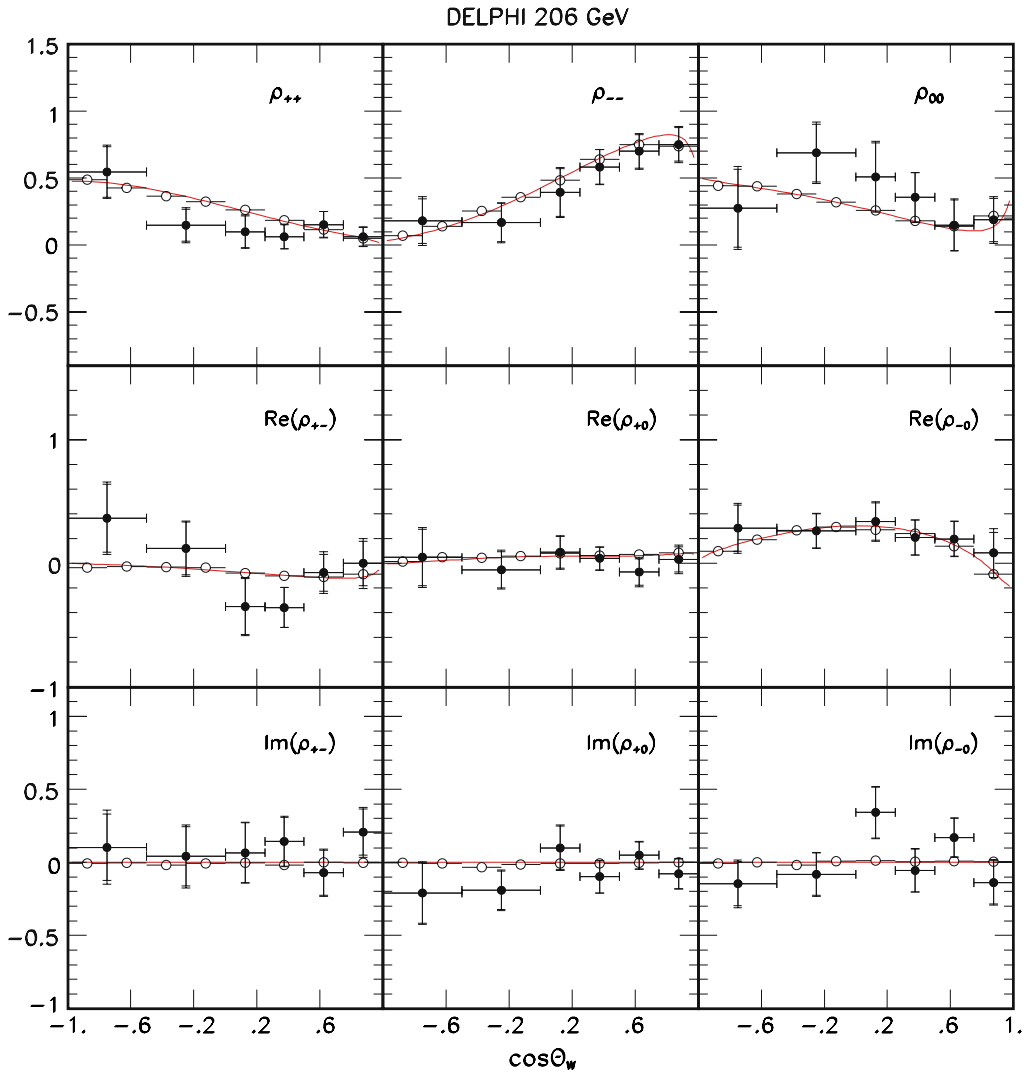

Fig. 11. Averages of W^+ and W^- SDM elements, with statistical and total errors, measured with the data taken at an energy of 206 GeV (*black dots*), corrected for detector acceptance and sample purity as explained in the text. The *full line* shows the tree level SM prediction calculated with the analytical expression from ref. [6]. The *open circles* are the SM tree level predictions obtained with the WPHACT MC at generator level

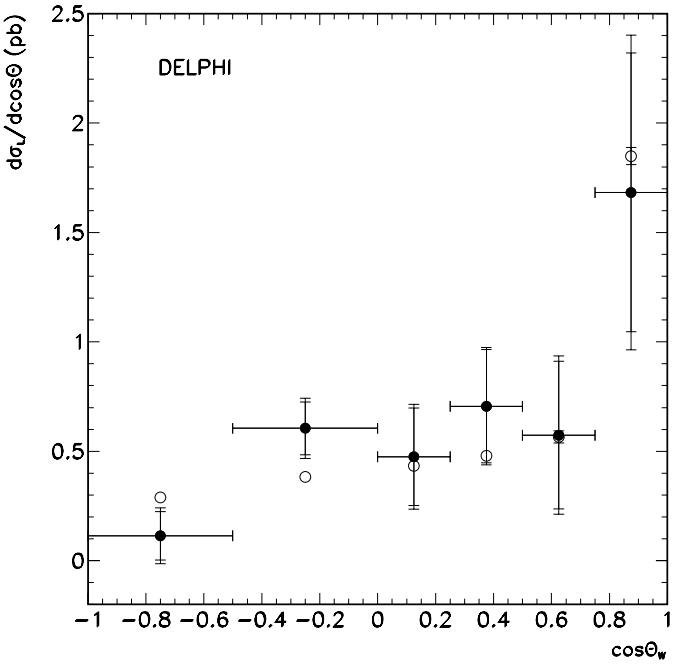

Fig. 12. Luminosity weighted average of the differential cross-sections measured at 189, 198 and 206 GeV (*black dots*) for longitudinally polarised W-bosons as a function of $\cos\Theta_W$, with statistical and total errors. The *open circles* show the values obtained from WPHACT MC at 199.5 GeV at generator level

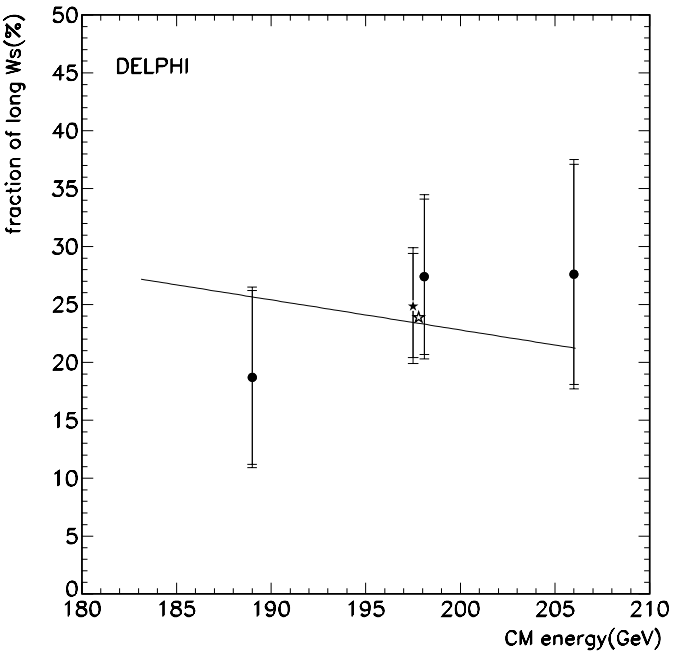

Fig. 13. Fraction of longitudinally polarised W-bosons as function of centre-of-mass energy, with statistical and total errors. The *black dots* represent the measurements and the *full line* the values obtained from WPHACT MC at generator level. The *black star* is the luminosity weighted mean of the measurements at the three energies and the *open star* the equivalent mean obtained from WPHACT MC at generator level as explained in the text

culated with simulated events at generator level and at reconstruction level, using the HERWIG hadronisation modelling [27], were computed. The reconstructed SDM elements were obtained by reweighting the selected events with the standard detector corrections obtained from the JETSET hadronisation modelling. The absolute values of these differences were taken as systematic uncertainty. This uncertainty was estimated at 199.5 GeV and the same value was used for all 3 energies. A problem with the track reconstruction efficiency for low-momentum particles at low polar angles was corrected for as described in [28]. We have investigated the systematic error related to this correction and found that it was negligible.

4. Cut on lepton polar angle. In the analysis, events with a lepton close to the beam (polar angle below 20° or above 160°) were rejected, and the standard detector corrections were calculated accordingly. To estimate the effect of the limited resolution in the reconstruction of the lepton angle, the analysis was redone with a cut at both 18° and 22°. The detector corrections were recalculated, one set for each cut, and the events were corrected with these new sets. The differences between the SDM elements obtained in the analysis with a cut at 22° and the analysis with a cut at 18° were rescaled to a difference corresponding to ±0.5°. This is a conservative estimate compared to the estimated value of the resolution which is about 0.1°, plus some tails. In addition, the SDM elements were recalculated with these new cuts, but corrected with the standard detector corrections, and the difference scaled down to ±0.5° was also computed. This yields two estimates of the uncertainty related to the resolution on the lepton polar angle reconstruction and the modelling of this reconstruction in the simulation. The larger estimate was taken as systematic uncertainty.
5. Cut on the χ^2 probability of the 3C fit. The analysis was redone with two different cuts on the χ^2 probability, at 0.003 and at 0.007, in a region where the probability has a flat distribution. For each cut, detector corrections were recalculated and the data were corrected with these new sets of corrections. The mean difference between the elements obtained with each new set of corrections and the standard elements was taken as systematic uncertainty.
6. Radiative corrections and CC03 reweighting. The purities which enter in the detector corrections refer to CC03 events of the type $e^+e^- \to W^+W^- \to l\nu q\bar{q}(l = e, \mu)$. The simulated event samples which were used to calculate these purities contain all four-fermion charged current processes. To obtain the signal angular distributions which are input to the purity calculations the events were reweighted with CC03 weights following the reweighting procedure explained in [25]. The uncertainty on the calculation of the radiative corrections has only a small influence on the SDM elements (see Sect. 3). The combined effect of the uncertainty from the CC03 reweighting and the radiative corrections was estimated by the difference between the analytical calculation of the SDM's used for the TGC fits

Table 2. Luminosity weighted average of the systematic error on ρ_{00} (average of W^- and W^+ elements) in the 6 $\cos\Theta_W$ bins with bin 1 being the most backward bin

$\cos\Theta_W$ bin	1	2	3	4	5	6
MC statistics	0.042	0.029	0.021	0.011	0.017	0.008
theoretical cross-sections	0.003	0.001	0.001	0.002	0.001	0.001
reconstruction	0.006	0.012	0.034	0.020	0.003	0.027
θ_{lepton} cut	0.026	0.007	0.005	0.009	0.016	0.017
Prob(χ^2) cut	0.021	0.023	0.027	0.007	0.017	0.008
radiat. corr. + CC03 rewgt	0.019	0.010	0.010	0.009	0.014	0.032
lepton charge	0.018	0.010	0.005	0.006	0.004	0.003
total systematic error	0.060	0.042	0.050	0.028	0.033	0.047

Table 3. Systematic error on f_{L} for the 3 energies and luminosity weighted average

Data set	189 GeV	198 GeV	206 GeV	average
MC statistics	0.010	0.011	0.014	0.007
theoretical cross-sections	0.001	0.002	0.002	0.002
reconstruction	0.015	0.015	0.015	0.015
θ_{lepton} cut	0.007	0.007	0.011	0.008
Prob(χ^2) cut	0.004	0.004	0.005	0.005
radiat. corr. + CC03 rewgt	0.007	0.010	0.016	0.011
lepton charge	0.002	0.001	0.003	0.002
total systematic error	0.021	0.023	0.029	0.022
statistical error	0.075	0.067	0.095	0.045

(CC03 in the zero width approximation, no radiative corrections at all, see [6]) and the SDM elements calculated at generator level with samples of simulated signal events corresponding to about 50 000 pb^{-1} (WPHACT MC). For the cases where the error on the Monte Carlo calculation was larger than this difference, this error was taken as systematic uncertainty.

7. Lepton charge determination. In the forward and backward regions of the detector the lepton charge is sometimes badly determined. To estimate this effect on the SDM elements, 10% of the events were artificially given a wrong charge and the elements were recalculated with standard detector corrections. From a study of two-lepton events [29] the fraction of leptons with a wrong charge assignment was estimated to be less than 1%. The uncertainty on the SDM elements from lepton charge determination was obtained from a rescaling by a factor 10 of the difference between the elements calculated with the 10% wrong charge data and the standard elements.

The systematic errors on the 9 SDM elements in a given bin at a given energy are fully correlated since the elements are determined from the same events. The systematic error from Monte Carlo statistics (1.) is uncorrelated between bins and energies. All other systematic errors are fully correlated between bins and energies. Therefore a luminosity weighted average of the values obtained at the three energies was used in the TGC fits, hence reducing the effects of statistical fluctuations.

The systematic errors on the differential cross-sections and the fraction of longitudinally polarised W-bosons were estimated with the same procedure as that used for the SDM elements. When computing the luminosity weighted average of these quantities all systematic errors were considered fully correlated between years, apart from the error from Monte Carlo statistics. The systematic error on the fraction f_{L} is given in Table 3.

5 Fits of triple gauge couplings

Both CP-conserving and CP-violating TGC's are determined in this analysis, which is however particularly suited to the determination of CP-violating couplings, whose existence would be revealed by non-zero imaginary parts of the SDM's. To investigate the possible existence of the anomalous CP-violating TGC's $g_4^Z, \tilde{\kappa}_Z, \tilde{\lambda}_Z$ in each of the three data samples defined in Table 1, the experimental values of the single W SDM elements $\rho^{W^-}_{\tau\tau'}(s, \cos\Theta_W)$ and $\rho^{W^+}_{\tau\tau'}(s, \cos\Theta_W)$ determined in each of the $\cos\Theta_W$ bins considered in this analysis were fitted to theoretical expressions derived in [6]. For CP-invariant interactions the relationship (6) holds. This allows a combination of W^- and W^+ elements in each $\cos\Theta_W$ bin. This procedure was applied in order to extract the CP-conserving couplings $\Delta g_1^Z, \Delta\kappa_\gamma$ and λ_γ.

In each of the $\cos\Theta_W$ bins the 9 SDM elements are correlated. The strongest correlations occur between

Table 4. Results of one-parameter fits including total (statistical and systematic) errors. In the last column, the errors on the results of fits to the full sample using only statistical errors on the SDM elements are given for comparison

Data set	189 GeV	198 GeV	206 GeV	full sample	
				fit result	stat. err.
Δg_1^Z	$0.12\ ^{+0.14}_{-0.21}$	$0.15^{+0.10}_{-0.14}$	$-0.53^{+0.48}_{-0.34}$	$0.07^{+0.08}_{-0.12}$	$^{+0.08}_{-0.10}$
χ^2/ndf	23/29	18/29	18/29	61/89	
λ_γ	$0.22\ ^{+0.29}_{-0.30}$	$0.16^{+.18}_{-.21}$	$0.09^{+0.14}_{-0.15}$	$0.16^{+0.12}_{-0.13}$	$^{+0.08}_{-0.09}$
χ^2/ndf	23/29	19/29	19/29	60/89	
$\Delta\kappa_\gamma$	$-0.31^{+0.55}_{-0.34}$	$-0.38^{+.25}_{-.22}$	$-0.27^{+0.28}_{-0.23}$	$-0.32^{+0.17}_{-0.15}$	$^{+0.16}_{-0.14}$
χ^2/ndf	23/29	17/29	18/29	58/89	
g_4^Z	-0.25 ± 0.32	$-0.50^{+0.29}_{-0.30}$	$-0.34^{+0.34}_{-0.38}$	$-0.39^{+0.19}_{-0.20}$	± 0.17
χ^2/ndf	141/95	108/95	80/95	330/287	
$\tilde{\kappa}_Z$	-0.01 ± 0.09	$-0.15^{+0.09}_{-0.06}$	$-0.10^{+0.20}_{-0.09}$	$-0.09^{+0.08}_{-0.05}$	$^{+0.06}_{-0.05}$
χ^2/ndf	142/95	109/95	81/95	333/287	
$\tilde{\lambda}_Z$	-0.01 ± 0.16	$-0.15^{+0.11}_{-0.12}$	$-0.04^{+0.11}_{-0.12}$	-0.08 ± 0.07	± 0.07
χ^2/ndf	142/95	109/95	81/95	333/287	

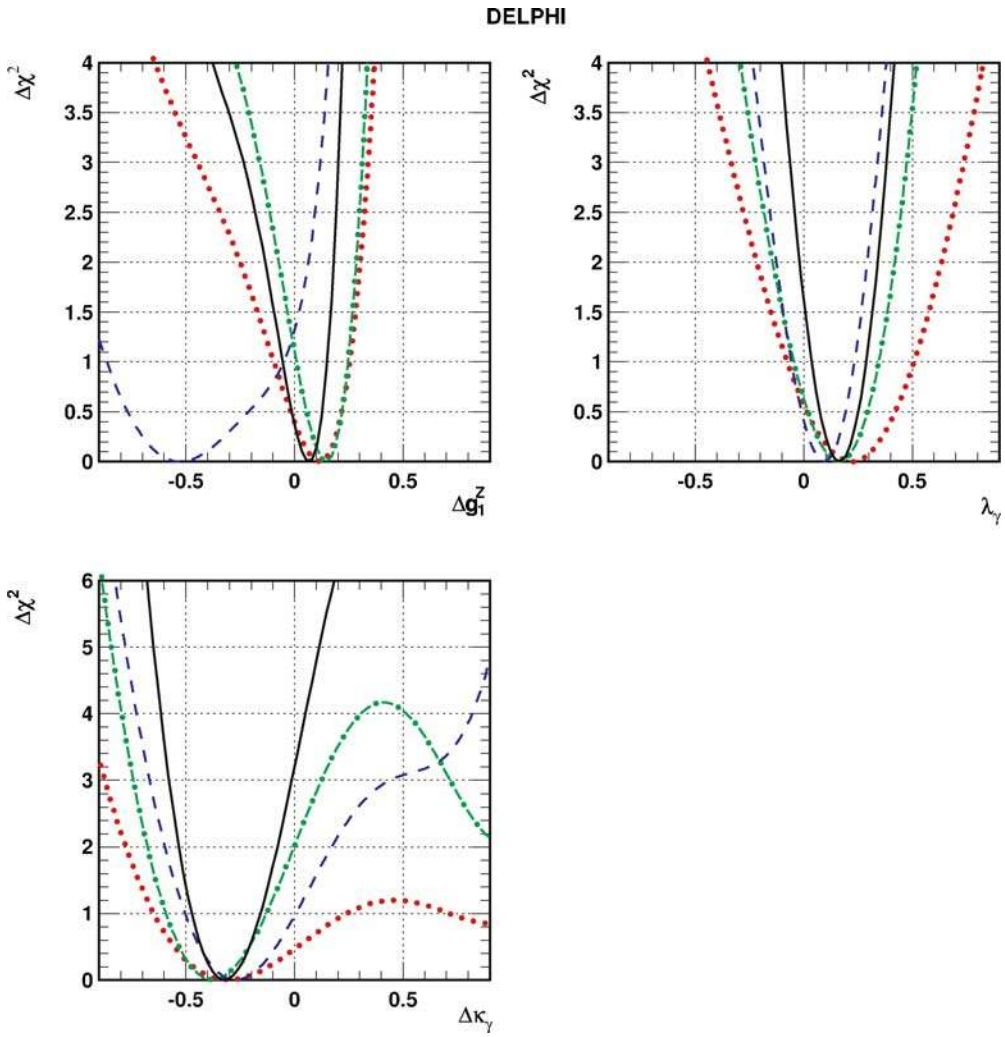

Fig. 14. Results of the one-parameter CP-conserving TGC fits. The *full line*s show the χ^2 curves for the full data sample, the *dotted lines* show the 189 GeV results, the *dash-dotted lines* show the results at 198 GeV and the *dashed lines* show the results at 206 GeV. Statistical and systematic errors are included. The results of the fits are displayed in Table 4

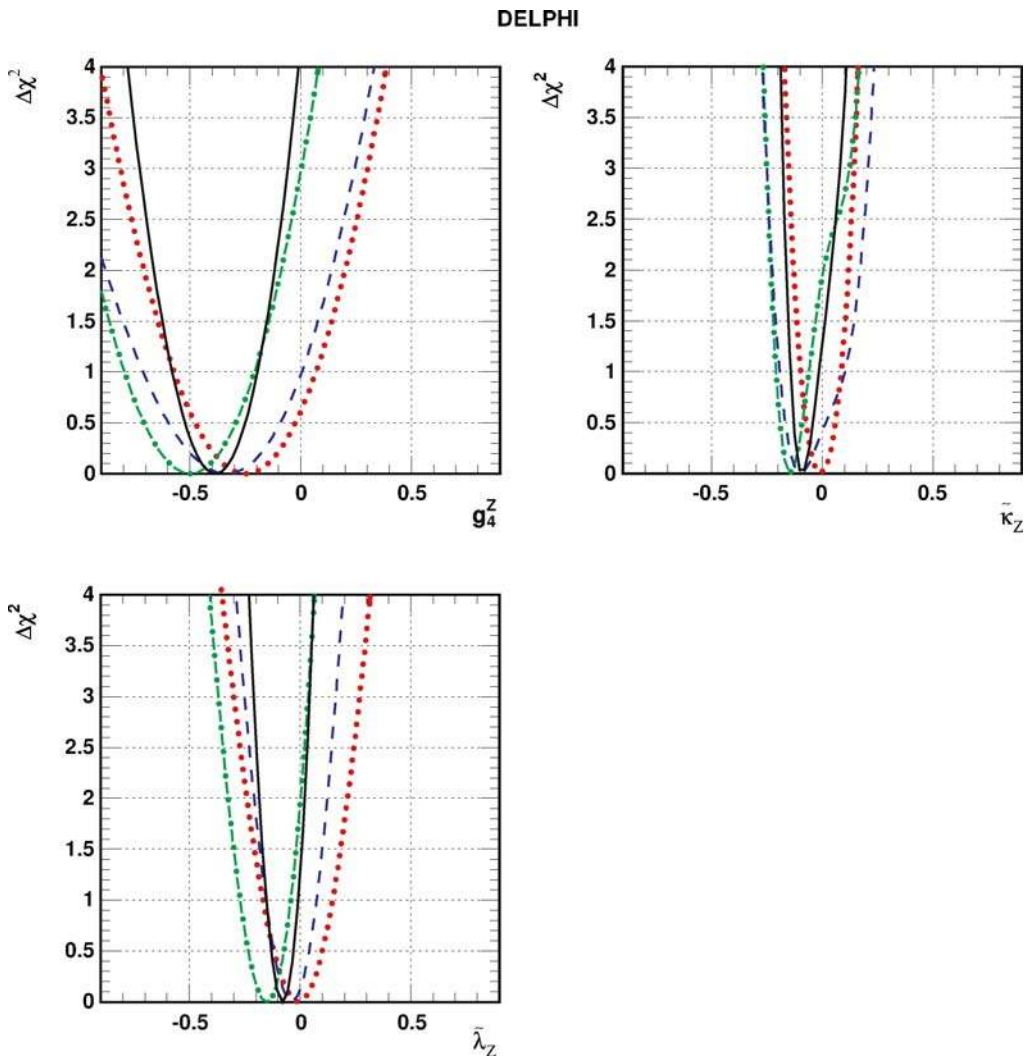

Fig. 15. Results of the one-parameter CP-violating TGC fits. The *full lines* show the χ^2 curves for the full data sample, the *dotted lines* show the 189 GeV results, the *dash-dotted lines* show the results at 198 GeV and the *dashed lines* show the results at 206 GeV. Statistical and systematic errors are included. The results of the fits are displayed in Table 4

ρ_{++}, ρ_{--} and ρ_{00}, whose sum is constrained to be one. The correlations were determined from the data and taken into account in the fit.

As the sum of the projection operators $\Lambda_{++} + \Lambda_{--} + \Lambda_{00} = 1$, it is seen from expression (9) that the sum of the experimentally determined diagonal SDM elements will always be exactly equal to one, whatever the sample used. The most straightforward way to take this constraint into account is to retain only two of the three diagonal elements in the fit, whose results are indeed totally insensitive to which of those elements is rejected. In the following, the element ρ_{++} has been removed from the fits which are hence reduced to five real SDM elements per bin $(\rho_{--}, \rho_{00}, \mathrm{Re}(\rho_{+-}), \mathrm{Re}(\rho_{+0}), \mathrm{Re}(\rho_{-0}))$ to determine the CP-conserving couplings, and to sets of 8 elements per bin (as above plus $\mathrm{Im}(\rho_{+-}), \mathrm{Im}(\rho_{+0}), \mathrm{Im}(\rho_{-0})$) for the extraction of the CP-violating couplings.

A least squares fit was used in which the measured values of the SDM elements were compared to their theoretical predictions at the average centre-of-mass energies for each of the three data sets. The statistical covariance matrices were computed from the data. These were combined with the full systematic covariance matrix containing the systematic errors described in Sect. 4.

Table 4 shows the results of the one-parameter fits for the three data sets separately and for the combined fit to all data. The total (statistical and systematic) error matrices were used. In each χ^2 fit only one of the TGC's considered was varied, all other couplings being fixed at their SM value. The χ^2 curves of the fits are displayed in Fig. 14 for the CP-conserving couplings and in Fig. 15 for the CP-violating couplings. The minimum χ^2 values are displayed in Table 4. The χ^2 probabilities of all fits to the full sample are acceptable, but are considerably lower for the CP-violating fits than for the CP-conserving fits. This is mainly due to the data at 189 GeV. The errors on the results of fits using only statistical errors on the SDM elements are given in the last column of Table 4.

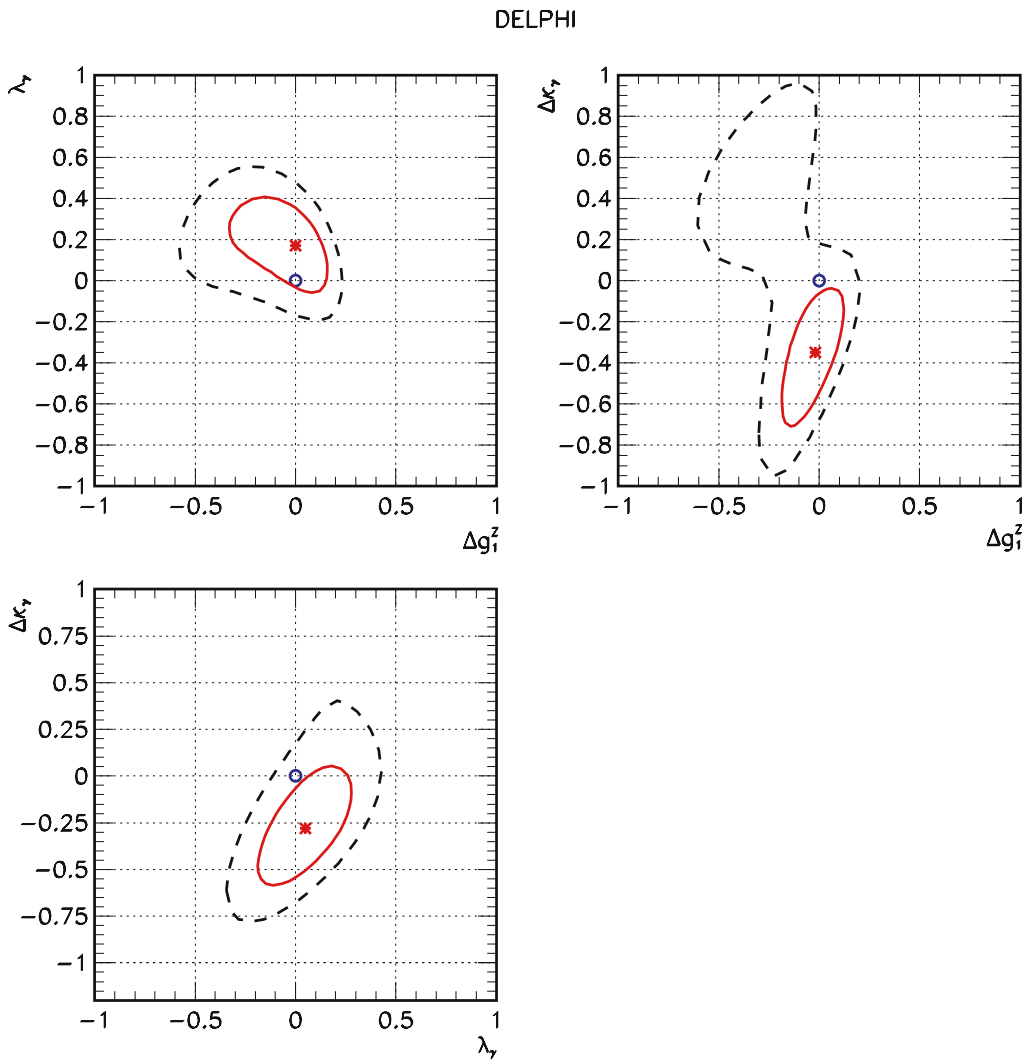

Fig. 16. Two-parameter CP-conserving TGC fits to the full data set. The *star* shows the fit results while the *open circle* represents the SM value. The *full line* shows the 68% CL contour and the *dashed line* the 95% CL contour. Statistical and systematic errors are included

It is seen that the results of the fits are dominated by the statistical errors. Using statistical errors only, the results of the Monte Carlo studies of 250 data-sized samples with SDM's computed at generation and at reconstruction level do not indicate any marked bias of the fitted values of the TGC's with respect to their SM input values. These Monte Carlo studies also revealed the existence of a double minimum in the fits of $\Delta\kappa_\gamma$ which is confirmed by the data, as seen in Fig. 14. Such double minima can occur [1, 30] as the helicity amplitudes are linear in the couplings.

In the fits to the data the average beam energies, displayed in Table 1 for each of the data taking years, were used. However, as already mentioned in Sect. 2, the beam energy of the data samples taken in 1999 varied from 192 to 202 GeV and from 204 to 209 GeV for the samples taken in the year 2000. The effect of these beam energy spreads on the errors on the fitted values of the TGC's was estimated by repeating the single parameter fits with beam energy values varying within the allowed energy ranges. The resulting shifts in the fitted values of the TGC parameters are very small and have been treated as systematic errors included in the full errors given in Table 4. The maximum size of this systematic error is 0.02.

Two-parameter fits of the TGC's at fixed central beam energy values were also performed, the results of which are shown in Figs. 16 and 17 for the full data set using the total (statistical and systematic) error matrix. The results are in reasonable agreement with the SM expectations. It is seen from Fig. 16 that the fit of $\Delta\kappa_\gamma$ exhibits a second minimum which appears as an extension of the 95% probability contour. This second minimum also strongly affects the shape of the $\Delta\chi^2$-plot at 189 GeV shown in Fig. 14.

Finally, three-parameter fits to the full data sample with full error matrices were also performed separately for the CP-conserving and CP-violating couplings respectively. The results are shown in Table 5, in which the errors shown are the standard deviations of the marginal distributions of each of the parameters.

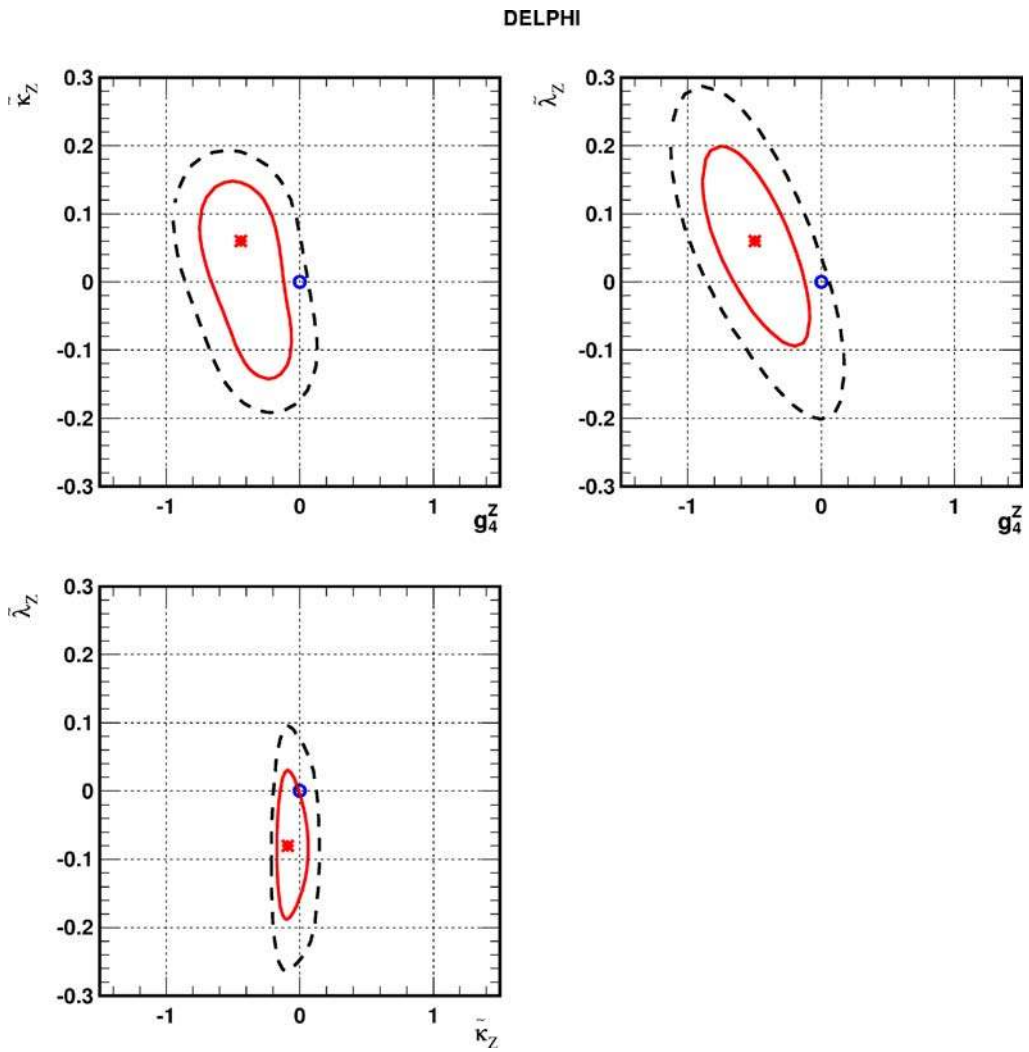

Fig. 17. Two-parameter CP-violating TGC fits to the full data set. The *star* shows the fit results while the *open circle* represents the SM value. The *full line* shows the 68% CL contour and the *dashed line* the 95% CL contour. Statistical and systematic errors are included

Table 5. Results of three-parameter fits (including the correlations between the fitted parameters) to the full sample. The errors are the total, statistical plus systematic, uncertainties. The χ^2 for the fits of the CP-conserving parameters (top) is 58 for 87 degrees of freedom. The χ^2 for the fits of the CP-violating parameters (bottom) is 329 for 285 degrees of freedom

	fitted value	Δg_1^Z	λ_γ	$\Delta\kappa_\gamma$
Δg_1^Z	$-0.03\ ^{+0.10}_{-0.11}$	1.00	−0.22	0.47
λ_γ	0.06 ± 0.16		1.00	0.45
$\Delta\kappa_\gamma$	$-0.31\ ^{+0.24}_{-0.25}$			1.00
	fitted value	g_4^Z	$\tilde{\kappa}_Z$	$\tilde{\lambda}_Z$
g_4^Z	-0.58 ± 0.27	1.00	−0.23	−0.66
$\tilde{\kappa}_Z$	$0.06\ ^{+0.07}_{-0.10}$		1.00	0.06
$\tilde{\lambda}_Z$	0.07 ± 0.09			1.00

The results of the one, two and three-parameters fits are consistent with each other and agree with the Standard Model.

6 Summary

The data taken by the DELPHI experiment at centre-of-mass energies of 189, 192–202 and 204–209 GeV were used to select a sample of respectively 520, 838 and 522 events of the type $e^+e^- \to l\nu q\bar{q}(l = e, \mu)$. The decay angles of the leptonically decaying W-bosons were used to calculate the single W^- and W^+ spin density matrices, which are defined for CC03 events, and the average values assuming CP symmetry.

The SDM elements were used to determine the fractions of longitudinally polarised W-bosons. For each of the three data samples the measured fraction of longitudinally polarised W-bosons is in agreement with the SM prediction.

For all data taken between 189 and 209 GeV an average value of

$$\sigma_{\rm L}/\sigma_{\rm tot} = 24.9 \pm 4.5({\rm stat}) \pm 2.2({\rm syst})\% \qquad (13)$$

is obtained at an average energy of 198 GeV, where $23.9 \pm 0.2\%$ is expected from the Standard Model.

The SDM elements have been used to determine the CP-violating triple gauge couplings. One-parameter fits to the full data sample yield:

$$g_4^Z = -0.39^{+0.19}_{-0.20}\,,$$
$$\tilde{\kappa}_Z = -0.09^{+0.08}_{-0.05}\,,$$
$$\tilde{\lambda}_Z = -0.08 \pm 0.07\,.$$

For the CP-conserving TGC's the results are:

$$\Delta g_1^Z = 0.07^{+0.08}_{-0.12}\,,$$
$$\lambda_\gamma = 0.16^{+0.12}_{-0.13}\,,$$
$$\Delta\kappa_\gamma = -0.32^{+0.17}_{-0.15}.$$

The errors quoted result from a quadratic combination of the statistical and systematic errors on the SDM elements.

For the CP-conserving TGC's the values obtained in this analysis are less precise than those measured in the DELPHI analysis using optimal observables [12, 13], but they confirm the good agreement of all the fitted couplings with the predictions of the Standard Model.

Acknowledgements. We are greatly indebted to our technical collaborators, to the members of the CERN-SL Division for the excellent performance of the LEP collider, and to the funding agencies for their support in building and operating the DELPHI detector.

We acknowledge in particular the support of Austrian Federal Ministry of Education, Science and Culture, GZ 616.364/2-III/2a/98, FNRS–FWO, Flanders Institute to encourage scientific and technological research in the industry (IWT) and Belgian Federal Office for Scientific, Technical and Cultural affairs (OSTC), Belgium, FINEP, CNPq, CAPES, FUJB and FAPERJ, Brazil, Ministry of Education of the Czech Republic, project LC527, Academy of Sciences of the Czech Republic, project AV0Z10100502, Commission of the European Communities (DG XII), Direction des Sciences de la Matière, CEA, France, Bundesministerium für Bildung, Wissenschaft, Forschung und Technologie, Germany, General Secretariat for Research and Technology, Greece, National Science Foundation (NWO) and Foundation for Research on Matter (FOM), The Netherlands, Norwegian Research Council, State Committee for Scientific Research, Poland, SPUB-M/CERN/PO3/DZ296/2000, SPUB-M/CERN/PO3/DZ297/2000, 2P03B 104 19 and 2P03B 69 23(2002-2004), FCT - Fundação para a Ciência e Tecnologia, Portugal, Vedecka grantova agentura MS SR, Slovakia, Nr. 95/5195/134, Ministry of Science and Technology of the Republic of Slovenia, CICYT, Spain, AEN99-0950 and AEN99-0761, The Swedish Research Council, Particle Physics and Astronomy Research Council, UK, Department of Energy, USA, DE-FG02-01ER41155, EEC RTN contract HPRN-CT-00292-2002.

We also want to thank J. Layssac for useful comments on the interpretation of the theoretical expressions.

References

1. G. Gounaris et al., Physics at LEP2, ed. by G. Altarelli, T. Sjöstrand, F. Zwirner, CERN 96-01 (1996), Vol 1, p. 525
2. K.J.F. Gaemers, G.J. Gounaris, Z. Phys. C **1**, 259 (1979)
3. K. Hagiwara et al., Nucl. Phys. B **282**, 253 (1987)
4. M.S. Bilenky et al., Nucl. Phys. B **409**, 22 (1993)
5. M.S. Bilenky et al., Nucl. Phys. B **419**, 240 (1994)
6. G. Gounaris et al., Int. J. Mod. Phys. A **8**, 3285 (1993)
7. OPAL Collaboration, G. Abbiendi et al., Phys. Lett. B **585**, 223 (2004)
8. L3 Collaboration, P. Achard et al., Phys. Lett. B **557**, 147 (2003)
9. G. Gounaris, D. Schildknecht, F.M. Renard, Phys. Lett. B **263**, 291 (1991)
10. ALEPH Collaboration, S. Schael et al., Phys. Lett. B **614**, 7 (2005)
11. DELPHI Collaboration, P. Abreu et al., Phys. Lett. B **423**, 194 (1998)
12. DELPHI Collaboration, P. Abreu et al., Phys. Lett. B **502**, 9 (2001)
13. DELPHI Collaboration, J. Abdallah et al., Measurement of Trilinear Gauge Boson couplings in e^+e^- collisions at LEP2, in preparation
14. L3 Collaboration, P. Achard et al., Phys. Lett. B **586**, 151 (2004)
15. OPAL Collaboration, G. Abbiendi et al., Eur. Phys. J. C **33**, 463 (2004)
16. OPAL Collaboration, G. Abbiendi et al., Eur. Phys. J. C **19**, 229 (2001)
17. DELPHI Collaboration, P. Aarnio et al., Nucl. Instrum. Methods A **303**, 233 (1991)
18. DELPHI Collaboration, P. Abreu et al., Nucl. Instrum. Methods A **378**, 57 (1996)
19. DELPHI Collaboration, J. Abdallah et al., Eur. Phys. J. C **34**, 127 (2004)
20. E. Accomando, A. Ballestrero, Comput. Phys. Commun. **99**, 270 (1997)
21. E. Accomando, A. Ballestrero, E. Maina, Comput. Phys. Commun. **150**, 166 (2003)
22. S. Jadach, B.F.L. Ward, Z. Was, Comput. Phys. Commun. **130**, 260 (2000)
23. T. Sjöstrand, PYTHIA 5.719/JETSET 7.4, Physics at LEP2, ed. by G. Altarelli, T. Sjöstrand, F. Zwirner, CERN 96-01 (1996), Vol 2, p. 41
24. T. Sjöstrand et al., Comput. Phys. Commun. **135**, 238 (2001)
25. A. Ballestrero et al., Comput. Phys. Commun. **152**, 175 (2003)
26. A. Denner et al., Reports of the Working Groups on Precision Calculations for LEP2 Physics, ed. by S. Jadach, G. Passarino, R. Pittau, CERN 2000-009
27. G. Marchesini et al., Comput. Phys. Commun. **67**, 465 (1992)
28. DELPHI Collaboration, J. Abdallah et al., Eur. Phys. J. C **46**, 295 (2006)
29. DELPHI Collaboration, J. Abdallah et al., Eur. Phys. J. C **45**, 589 (2006)
30. R.L. Sekulin, Phys. Lett. B **338**, 369 (1994)